Monoacylglycerol Lipase Inhibition in Human and Rodent Systems Supports Clinical Evaluation of Endocannabinoid Modulators

Jason R. Clapper, Cassandra L. Henry, Micah J. Niphakis, Anna M. Knize, Aundrea R. Coppola, Gabriel M. Simon, Nhi Ngo, Rachel A. Herbst, Dylan M. Herbst, Alex W. Reed, Justin S. Cisar, Olivia D. Weber, Andreu Viader, Jessica P. Alexander, Mark L. Cunningham, Todd K. Jones, Iain P. Fraser, Cheryl A. Grice, R. Alan B. Ezekowitz, Gary P. O'Neill and Jacqueline L. Blankman*

Abide Therapeutics, 10835 Road to the Cure, Suite 250, San Diego, CA 92121, USA (J.R.C., C.L.H., M.J.N., A.M.N., A.R.C., G.M.S., N.N., R.A.H., D.M.H., A.W.R., J.S.C., O.D.W., A.V., J.P.A., M.L.C., T.K.J., I.P.F., C.A.G., R.A.B.E., G.P.O., J.L.B.).

Running Title:

Pharmacological characterization of MGLL inhibitor ABD-1970

***Corresponding author:**

Jacqueline L. Blankman, Ph.D.

Abide Therapeutics

10835 Road to the Cure, Suite 250

San Diego, CA 92121, USA

Tel.: +1 (858) 427-2590

Fax.: +1 (858) 716-0244

jackie@abidetx.com

Text pages: 60/38 (with/without references, footnotes and figures legends, respectively)

Tables: 1

Figures: 7 (+4 supplementary figures)

References: 69

Abstract: 199 words

Introduction: 724 words (including references)

Discussion: 1,461 words (including references)

List of non-standard abbreviations:

2-AG, 2-arachidonoylglycerol; 6k-$PGF_{1\alpha}$, 6-ketoprostaglandin F1α; AA, Arachidonic acid; AA-d_8, Arachidonic acid-d_8; ABD-0038, 3-(5-chloro-2-(piperazin-1-ylmethyl)phenyl)-8-oxa-3-azabicyclo[3.2.1]octane; ABD-1970, 1,1,1,3,3,3-hexafluoropropan-2-yl 4-(2-(8-oxa-3-azabicyclo[3.2.1]octan-3-yl)-4-chlorobenzyl)piperazine-1-carboxylate; ABHD6, Alpha/beta hydrolase-domain containing 6; ABPP, Activity-based protein profiling; ANOVA, Analysis of variance; CB1, Cannabinoid receptor 1; CB2, Cannabinoid receptor 2; CCI, Chronic constriction injury; CES1, Carboxylesterase 1; CFA, Complete Freund's adjuvant; CNS, Central nervous system; COX, Cyclooxygenase enzyme; DDA, data-dependent acquisition; DMEM, Dulbecco's modified Eagle's medium; DMSO, Dimethyl sulfoxide; ED_{50}, median effective dose; EDTA, Ethylenediaminetetraacetic acid; ESI, electrospray ionization; FAAH, Fatty acid amide hydrolase; FCS, Fetal calf serum; FP-biotin, [10-[[5-[[5-[(3aS,4S,6aR)-Hexahydro-2-oxo-1H-thieno[3,4-d]imidazol-4-yl]-1-oxopentyl]amino]pentyl]amino]-10-oxodecyl]phosphonofluoridic Acid Ethyl Ester; 10-Fluoroethoxyphosphinyl-N-biotinamidopentyldecanamide; FP-rh, rhodamine-tagged fluorophosphonate or 9-{2-carboxy-4-[(5-{14-[ethoxy(fluoro)phosphoryl]-2-oxo-3,6,9,12-tetraoxa-1-azatetradecan-1-yl}pentyl)carbamoyl]phenyl}-6-(dimethylamino)-N,N-dimethyl-3H-xanthen-3-iminium; HEK293T, Human embryonic kidney 293 cells containing the SV40 T-antigen; HUVEC, Human umbilical vein endothelial cells; IL-1β, Interleukin-1 beta; IRB, Institutional review board; LC, Liquid chromatography; LC-MS, liquid chromatography-mass spectrometry; LC-MS/MS, Liquid chromatography tandem mass spectrometry; LPS, Lipopolysaccharide; MGLL, Monoacylglycerol lipase (also known as MAG lipase, MAGL and

MGL); MRM, multiple-reaction-monitoring; MS, Mass spectrometry; NAL, Naltrexone; NSAID, Non-steroidal anti-inflammatory drug; PBMC, Peripheral blood mononuclear cells; PBS, Phosphate-buffered saline; PC3, Human prostate carcinoma cells; PD, Pharmacodynamic; PDA, Pentadecanoic acid; PEG400, Polyethylene Glycol 400; PG, pregabalin; PGD_2, Prostaglandin D2; PGE_2, Prostaglandin E2; $PGF_{2\alpha}$, Prostaglandin F2α; PK, Pharmacokinetic; PLA2G7, Platelet-activating factor acetylhydrolase; PO, oral gavage; RPMI, Roswell Park Memorial Institute medium; SDS, Sodium dodecyl sulfate; SDS-PAGE, Sodium dodecyl sulfate polyacrylamide gel electrophoresis; SEM, Standard error of the mean; SIM, single ion monitoring; SC, subcutaneous; TCEP, tris(2-carboxyethyl)phosphine; THC, Tetrahydrocannabinol; TSRI, The Scripps Research Institute; TXB_2, Thromboxane B2; WIN 55,212-2, (*R*)-(+)-[2,3-Dihydro-5-methyl-3[(4-morpholinyl)methyl]pyrrolo[1,2,3-de]-1,4-benzoxazinyl]-(1-naphthalenyl)methanone mesylate salt.

Recommended section assignment: Drug Discovery and Translational Medicine

JPET Fast Forward. Published on October 10, 2018 as DOI: 10.1124/jpet.118.252296
This article has not been copyedited and formatted. The final version may differ from this version.

ABSTRACT

Monoacylglycerol lipase (MGLL) is the primary degradative enzyme for the endocannabinoid 2-arachidonoylglycerol (2-AG). The first MGLL inhibitors have recently entered clinical development for the treatment of neurological disorders. To support this clinical path, we report the pharmacological characterization of the highly potent and selective MGLL inhibitor ABD-1970 (1,1,1,3,3,3-hexafluoropropan-2-yl 4-(2-(8-oxa-3-azabicyclo[3.2.1]octan-3-yl)-4-chlorobenzyl)piperazine-1-carboxylate). We used ABD-1970 to confirm the role of MGLL in human systems and to define the relationship between MGLL target engagement, brain 2-AG concentrations and efficacy. As MGLL contributes to arachidonic acid (AA) metabolism in a subset of rodent tissues, we further used ABD-1970 to evaluate whether selective MGLL inhibition would affect prostanoid production in several human assays known to be sensitive to cyclooxygenase (COX) inhibitors. ABD-1970 robustly elevated brain 2-AG content and displayed antinociceptive and anti-pruritic activity in a battery of rodent models (ED_{50} values of 1-2 mg/kg). The antinociceptive effects of ABD-1970 were potentiated when combined with analgesic standards of care and occurred without overt cannabimimetic effects. ABD-1970 also blocked 2-AG hydrolysis in human brain tissue and elevated 2-AG content in human blood without affecting stimulated prostanoid production. These findings support the clinical development of MGLL inhibitors as a differentiated mechanism to treat pain and other neurological disorders.

INTRODUCTION

Monoacylglycerol lipase (MGLL, also known as MAG lipase, MAGL and MGL) is a serine hydrolase enzyme that regulates endocannabinoid and eicosanoid families of lipid signaling molecules (Grabner et al., 2017). MGLL catalyzes the hydrolysis of 2-arachidonoylglycerol (2-AG), an endogenous ligand of the cannabinoid receptors 1 and 2 (CB1 and CB2) (Mechoulam et al., 1995; Sugiura et al., 1995), effectively terminating 2-AG signaling (Long et al., 2009a). In the nervous system, post-synaptic activity stimulates the biosynthesis and mobilization of 2-AG, which then traverses the synaptic cleft in a retrograde manner to agonize pre-synaptically localized CB1 (Kano et al., 2009; Katona and Freund, 2008). CB1 activation reduces the probability of neurotransmitter release, thus serving as a natural brake for excessive neurotransmission in active circuits (Kano et al., 2009). MGLL is co-localized with CB1 in presynaptic neurons (Gulyas et al., 2004; Katona et al., 2006) and in neighboring glia (Viader et al., 2015), positioning the enzyme to exert tight control of 2-AG signaling.

Direct pharmacological activation of the CB receptors by *Cannabis* preparations, tetrahydrocannabinol (THC) and synthetic cannabinoids can elicit therapeutically beneficial effects on pain, spasticity, appetite, and nausea (Pertwee, 2012); however, dose-limiting central nervous system (CNS) effects of such exocannabinoids limit their broad use as pharmaceuticals. An alternative strategy to exocannabinoids is amplification of endocannabinoid signaling through inhibition of endocannabinoid degradation. MGLL is the major 2-AG hydrolase in the CNS and most peripheral tissues, and genetic or pharmacological inactivation of this enzyme reduces 2-AG hydrolysis and elevates tissue 2-AG concentrations in rodents (Chanda et al., 2010; Long et al., 2009b; Schlosburg et al., 2010). MGLL inhibitors produce an array of CB1/2-

mediated effects in animal models, including antinociceptive (Grabner et al., 2017), anxiolytic (Bedse et al., 2018; Patel et al., 2017), and anti-epileptogenic effects (Griebel et al., 2015; Sugaya et al., 2016; von Ruden et al., 2015), without inducing the full spectrum of stereotypical behaviors observed following administration of direct CB1 agonists (Ignatowska-Jankowska et al., 2015; Ignatowska-Jankowska et al., 2014; Long et al., 2009b). These observations may reflect that MGLL inhibitors potentiate ongoing 2-AG signaling while preserving the spatial and temporal specificity of the endocannabinoid system, unlike exocannabinoids, which indiscriminately activate CB1 throughout the brain.

The product of MGLL-mediated 2-AG hydrolysis, arachidonic acid (AA), is the precursor for prostanoid signaling molecules (Funk, 2001). MGLL-mediated 2-AG hydrolysis serves as one of the sources of AA in the rodent nervous system (Long et al., 2009b) and contributes to brain levels of pro-inflammatory prostanoids (Nomura et al., 2011). MGLL inactivation in mice reduces molecular and cellular signs of neuroinflammation and is protective in models of neurodegeneration and status epilepticus, through CB-independent mechanisms, suggesting involvement of prostanoid suppression (Chen et al., 2012; Nomura et al., 2011; Piro et al., 2012; Terrone et al., 2018; Zhang and Chen, 2018). The contribution of MGLL to AA metabolism in the mouse is tissue-dependent (Nomura et al., 2011). This anatomical segregation suggests that inhibition of MGLL may afford some of the anti-inflammatory effects associated with a reduction in prostanoid signaling without the side effects caused by non-steroidal anti-inflammatory drugs (NSAID) or coxibs, which reduce prostanoid signaling through the inhibition of COX1 and/or COX2 enzymes. In rodents, MGLL inhibition is devoid of gastrointestinal effects and, instead, protects from NSAID-induced gastric hemorrhages via CB1 (Crowe and Kinsey, 2017; Kinsey et al., 2011). The effects of MGLL blockade on prostaglandin

production and signaling in human cellular systems have, to our knowledge, not been reported, but could potentially further differentiate MGLL inhibitors from COX1/2 inhibitors.

To support clinical investigation of endocannabinoid modulation, we report herein the pharmacological characterization of an advanced compound ABD-1970 (Cisar et al., 2018) that serves as a highly potent and selective MGLL inhibitor. We show that oral administration of ABD-1970 to rodents leads to potent and sustained inhibition of MGLL and accumulation of 2-AG in the brain, which is accompanied by dose-dependent antinociceptive and anti-pruritic activity. The antinociceptive effects of ABD-1970 combine beneficially with analgesic standards of care and occur without overt cannabimimetic effects. Studies with ABD-1970 confirm that MGLL is a principle regulator of 2-AG in human brain and demonstrate that in stimulated human blood and endothelial cells, blockade of this enzyme does not affect prostanoid production, and thus clearly differentiates from COX inhibition. Together, these results support the pursuit of MGLL inhibitors for the safe and differentiated treatment of neurological disorders in humans.

MATERIAL AND METHODS

Drugs and reagents

ABD-1970 was synthesized at Abide Therapeutics, as previously described (Cisar et al., 2018). Synthesis of the potential hydrolysis product ABD-0038 (3-(5-chloro-2-(piperazin-1-ylmethyl)phenyl)-8-oxa-3-azabicyclo[3.2.1]octane) was performed at Abide Therapeutics and is described in the Supplemental Methods. The rhodamine-tagged fluorophosphonate (FP-Rh) (Patricelli et al., 2001), FP-biotin (Jessani et al., 2005), HT-01 (Hsu et al., 2012) and JW912

JPET Fast Forward. Published on October 10, 2018 as DOI: 10.1124/jpet.118.252296
This article has not been copyedited and formatted. The final version may differ from this version.

(Chang et al., 2013) activity-based probes were synthesized at Abide Therapeutics, as previously described. Other drugs and reagents were obtained as follows: CFA from Chondrex Inc (Redmond, WA), buprenorphine from China Resources Pharmaceutical Commercial Group Co. (Beijing, China), morphine from Johnson Matthey MacFarlan Smith (Edinburgh, UK), pregabalin from Sequoia (Pangbourne, UK) or Pfizer (Lyrica™ 50 mg capsules, Lot J30252), and WIN 55,212-2 from Tocris Bioscience (Bristol, UK). Lipids, deuterated lipid standards, indomethacin and rofecoxib were purchased from Cayman Chemical (Ann Arbor, MI). All other reagents were obtained from Sigma, unless stated otherwise. For *in vitro* studies, drugs were dissolved in dimethyl sulfoxide (DMSO). For *in vivo* studies, drugs were prepared daily in 0.5% methylcellulose (w/v), 7:2:1: PEG400/ethanol/PBS (v/v/v), 0.9% saline, or 1% Tween 80/99% saline (v/v), as specified in the relevant method sections.

Biochemical studies

Determination of inhibitor potency and selectivity by activity-based protein profiling (ABPP). The potency and selectivity of ABD-1970 were assessed by competitive ABPP using sodium dodecyl sulfate polyacrylamide gel electrophoresis (SDS-PAGE) (Simon and Cravatt, 2010) in membrane homogenates prepared from male mouse, rat, rabbit, dog, monkey and human brain tissue, human prostate carcinoma cells (PC3) (ATCC, Manassas, VA; CRL-1435, mycoplasma negative), and peripheral blood mononuclear cells (PBMC) isolated from human whole blood. ABPP selectivity profiling was also performed in total homogenates prepared from human brain, liver, kidney, skin, lung and PBMC. The activity of the potential hydrolysis product ABD-0038 was evaluated in mouse, rat and human brain homogenates. A detailed

description of the preparation of tissue homogenates and cell lysates is provided in the Supplemental Methods.

Gel-based ABPP analysis was performed as described previously (Leung et al., 2003) using three ABPP probes: FP-Rh probe (Patricelli et al., 2001), HT-01 (Hsu et al., 2012) and JW912 (Chang et al., 2013). Brain membrane homogenates (50 μg), PC3 membrane lysates (100 μg), PC3 cells (100 mm dishes), human tissue homogenates (50 μg), or human whole blood (4 mL) were treated with ABD-1970 or DMSO for 30 minutes at 37°C. Lysates were prepared from compound-treated PC3 cells and PBMC were isolated from compound-treated whole blood, as described in the Supplemental Methods. ABPP analysis was performed by treating the tissue or cell homogenates with 1 μM FP-Rh (all tissue homogenates and PBMC), HT-01 (rodent and dog brain homogenates) or JW912 (PC3 membranes) for 30 minutes at 25°C. Reactions were quenched with 4X SDS-PAGE loading buffer, separated by SDS-PAGE (10% acrylamide) and fluorescence was visualized in-gel with a Bio-Rad ChemiDox™ XRS fluorescence imager. Fluorescence is shown in gray scale. Quantitation of fluorescent band intensities was performed by densitometric analysis using ImageJ software version 1.5 (NIH, Bethesda, MD). Integrated peak intensities were generated for bands corresponding to MGLL activity (labeled with FP-Rh or JW912) or alpha/beta hydrolase-domain containing 6 (ABHD6) activity (labeled with HT-01 or JW912). IC_{50} values were calculated by curve fitting semi-log transformed data (x-axis) by non-linear regression with a 4-parameter, sigmoidal dose response function (variable slope) in Prism software version 6 (GraphPad, La Jolla, CA).

Quantitative mass spectrometry (MS)-based ABPP was used to profile the selectivity of ABD-1970 in human brain homogenates using the FP-biotin probe. Human prefrontal cortex

membrane homogenates were treated with 0.01-10 μM ABD-1970 or DMSO for 30 minutes at 37°C. Samples were treated with FP-biotin, enriched by avidin chromatography and digested by trypsin, essentially as previously described (Jessani et al., 2005). Tryptic digests of the inhibitor- and DMSO-treated samples were isotopically labeled by reductive dimethylation of primary amines with natural or isotopically heavy formaldehydes (Boersema et al., 2009) and subsequently analyzed by liquid chromatography tandem mass spectrometry (LC-MS/MS) on a Thermo Fisher (Waltham, MA) Velos Elite Orbitrap mass spectrometer. Peptide spectral matching was performed with the complete human UniProt database using the ProLuCID algorithm (version 1.3.3), and the resulting matches filtered using DTASelect (version 2.0.47). Quantification of light/heavy ratios was performed using the Cimage algorithm. Data were plotted as percent inhibition relative to DMSO-treated samples. Full details can be found in the Supplemental Methods.

Determination of inhibitor potency by substrate assays. 2-AG hydrolysis activity in human brain cortex membrane homogenates (20 μg in 200 μL PBS) treated with ABD-1970 or DMSO vehicle (30 min at 37°C) was assessed using a MS-based substrate assay, essentially as previously described (Blankman et al., 2007). Full experimental details can be found in the Supplemental Methods.

The potency of ABD-1970, independent of preincubation time, was determined as the k_{inact}/K_i using purified recombinant human MGLL protein and a fluorogenic substrate assay. Full-length human MGLL was expressed in *Escherichia coli* bacteria with an N-terminal hexahistidine tag (Evotec, Watertown, MA), purified by NiNTA affinity chromatography followed by size exclusion chromatography (Evotec, Watertown, MA), and stored in 20 mM

Tris, pH 8.0, 100 mM NaCl and 10% glycerol. To initiate the assay, MGLL (4 nM) was added to the assay system consisting of ABD-1970 (62.5 to 3000 nM), 10 μM butyl resorufin substrate (Sigma), 200 mM KCl, 1 mM EDTA, 50 mM Hepes (pH 7.0) in a total volume of 100 μL. Reactions without enzyme or inhibitor were included as controls. Immediately following addition of MGLL protein, fluorescence was measured in a Biotek (Winooski, VT) Neo2 multimode meter set for excitation at 530 nm and emission at 587 nm. Data was collected at room temperature over 10 min, with individual reads every 12-13 s. The MGLL-dependent hydrolysis of the butyl resorufin substrate was monitored continuously to provide a progress curve for the rate of enzyme inactivation at varying inhibitor concentrations. The progress curve data was corrected by subtracting the average of four reactions run without enzyme. Non-linear fitting (GraphPad Prism) of these corrected progress curves to a single exponential equation ($Y = Y_0 + ((\text{plateau} - Y_0) * (1 - \exp(-K_{obs} * x)))$) provided the first-order rate constant, k_{obs}, at each concentration of inhibitor tested. The k_{obs} value was plotted against ABD-1970 concentration and the curve was fit using the equation: $k_{obs} = k_{inact}[I] / ([I] + K_i^{app})$ to obtain k_{inact} and K_i^{app}. The true K_i was subsequently calculated using the equation: $K_i^{app} = K_i(1 + [S]/K_m)$ (Copeland, 2000). Each experiment was performed with quadruplicate assay points and the entire experiment was repeated three times.

In vitro reversibility of inhibition and recovery of activity in cultured cells. The persistence of inhibition of human MGLL by ABD-1970 in vitro was evaluated following removal of free compound by multiple rounds of centrifugation. Human embryonic kidney 293 cells containing the SV40 T-antigen (HEK293T) were grown in Dulbecco's modified Eagle's medium (DMEM, Gibco) containing 10% fetal calf serum (FCS, Omega Scientific) at 37°C under 5% CO_2 to ~60% confluency and transfected with full-length human MGLL with an N-terminal FLAG epitope tag

or an empty vector (pFLAG-CMV-6b) using the Fugene 6 reagent (Promega, Madison, WI). After 48 hours, cell membrane lysates were prepared as described in the Supplemental Methods, and an aliquot (490 μg in 490 μL PBS) was treated with 1 μM ABD-1970 (10 μL of 50 μM) or DMSO for 30 min at 37°C. Cell lysates were subjected to two rounds of centrifugation (100,000 x g for 30 minutes at 4°C) and the membrane lysates were collected immediately (time = 0 hours), after 8 hours and after 24 hours at room temperature, and rapidly frozen on dry ice. Enzymatic activity of human MGLL was assessed in these samples after resuspending in PBS to 1 mg/mL using gel-based ABPP with the FP-Rh probe.

The recovery of MGLL activity in cultured human PC3 cells was evaluated following treatment with ABD-1970 and removal of free compound. PC3 cells were grown to 70-80% confluency in F-12K medium (Gibco, Grand Island, NY) supplemented with 10% FCS at 37°C with 5% CO_2, washed twice with PBS, and then incubated for 30 min at 37°C with serum-free cell culture medium containing ABD-1970 (10 nM) or DMSO (0.01% final concentration). Cells were washed with PBS to remove unbound ABD-1970, fresh media containing 10% FCS was added, and cells were incubated at 37°C with 5% CO_2 for up to 72 hours. Cells were harvested at 0.5, 6, 24, 48 and 72 hours following the removal of ABD-1970 and cell lysates were prepared. MGLL activity in ABD-1970 or DMSO treated PC3 lysates was then assessed using gel-based ABPP analysis with the JW912 probe. The average recovery rate of MGLL activity was calculated by linear regression analysis using Prism software (GraphPad, La Jolla, CA). The slope of the fit gave the average MGLL activity recovery rate in % MGLL activity per hour.

***In vivo* studies**

All animal experiments at Abide Therapeutics were performed in accordance with the guidelines outlined by the Guide for the Care and Use of Laboratory Animals and the Animal Welfare Act and approved by the Explora Biolabs Institutional Animal Care and Use Committee. Animal experiments carried out at external institutions were performed in accordance with the individual institutions and their respective country's policies governing the ethical and humane treatment of laboratory animals. In all studies, animals were maintained under a 12 hour light/dark cycle and allowed free access to food and water throughout the duration of the experiments.

Dose and time course effects of ABD-1970 in rodents: Male ICR mice (Envigo, Livermore, CA) and male Sprague Dawely rats (Charles River, Wilmington, MA) 6 to 10 weeks old at the time of dosing were administered ABD-1970 by oral gavage (5 mL/kg volume). ABD-1970 was prepared fresh on the day of dosing in 0.5% methylcellulose (400cP, Sigma-Aldrich, St Louis, MO) vehicle for the rat dose response study or in 7:2:1 PEG400:ethanol:PBS vehicle for the rat time course and mouse studies. Maximal dispersal of the compound was achieved by bath and probe sonication until a fine white suspension was formed. Animals were administered single oral doses of ABD-1970 (0.1 – 30 mg/kg for mice and 0.1 – 10 mg/kg for rats). At specified time points after ABD-1970 administration, animals were anesthetized with isoflurane, and blood samples were collected by cardiac puncture into syringes pre-coated with EDTA (500 mM disodium, Teknova, Hollister, CA). Following blood collection, animals were killed by decapitation, and brains were removed and rinsed in PBS before freezing in liquid nitrogen. One brain hemisphere was submitted for ABD-1970 concentration analysis by LC-MS/MS, and the other hemisphere was further dissected to remove 2 adjacent forebrain sections (~100-200 mg) and submitted for analysis of MGLL inhibition by ABPP with the FP-Rh probe, as described above, and for brain lipid concentrations by LC-MS/MS, as described below.

Due to the instability of ABD-1970 in rodent blood and plasma that is thought to be a consequence of CES enzymes, which are known to metabolize ester and carbamate xenobiotics, and are more abundant in rodent plasma than other higher mammal species, including dogs, primates, and humans (Berry et al., 2009), blood samples were immediately placed into an equal volume of acetonitrile to stabilize ABD-1970. After mixing, the samples were centrifuged (17,000 x g for 2 min), and the resulting whole blood supernatants were transferred and submitted to LC-MS/MS analysis for whole blood ABD-1970 measurements.

Brain lipid analysis. Quantitation of endocannabinoid and eicosanoid lipids in brain tissue following organic extraction was performed by LC-MS/MS analysis on an Agilent 1260 LC system coupled to an Agilent 6460 Triple Quadrupole mass spectrometer. Full experimental details are presented in the Supplemental Methods.

Formalin pain model: Male Sprague Dawley rats (171 – 235 g at the time of dosing, Harlan, UK) were administered an intraplantar injection of formalin (50 µL, 2.5%) into the dorsal surface of the right hindpaw to induce acute pain (Saretius Ltd., UK). Immediately after, paw licking behavior, a correlate of spontaneous pain (Abbott et al., 1995), was tracked using the Laboras™ (Laboratorium Animal Behaviour Observation, Registration and Analysis System, Metris B. V. Hoofddorp, The Netherlands) automated rodent behavioral tracking system, which was validated to differentiate and automatically recognize behaviors and locomotor activity of individually housed rats. Animals injected with formalin are immediately placed into the Laboras™ cages (22.5 cm (width) x 42.5 cm (length) x 19.0 cm (height)) and duration of paw licking behavior (in sec) was collected from two distinctive phases, the early nociceptive phase

occurring 0-5 min after formalin injection and the late phase thought to be associated with central sensitization, which peaks 10-30 min after formalin injection.

To establish a pharmacokinetic/pharmacodynamic (PK/PD) relationship, animals were administered vehicle (0.5% methylcellulose), ABD-1970 (1, 3, and 10 mg/kg) or the positive control pregabalin (60 mg/kg) 240 min before formalin injection. Forty-five minutes after formalin injection and behavioral monitoring, and approximately 285 min after treatment animals were anesthetized with isoflurane, and blood samples were collected by cardiac puncture. Following blood collection, animals were killed by decapitation and brains were removed. Samples were dissected and processed as described above for analysis of MGLL inhibition by ABPP and ABD-1970 and 2-AG concentrations by LC-MS/MS.

For the ABD-1970 and pregabalin combination study, male Sprague Dawley rats (214 - 235 g, Harlan, UK) were administered ABD-1970 (2 mg/kg) by oral gavage (5 mL/kg volume) immediately followed by a separate oral administration (5 mL/kg volume) of pregabalin (10 mg/kg) 240 min before formalin administration. For the monotherapy control groups, ABD-1970 or pregabalin were administered along with separate oral gavage administrations of vehicle (0.5% methylcellulose). Paw licking behavior was monitored for 30 min using the Laboras™ behavior tracking system. For the ABD-1970 and morphine combination study, male Sprague Dawley rats (225 – 269 g at the time of dosing, Harlan, UK) were administered vehicle (0.5% methylcellulose) or ABD-1970 (1 mg/kg) by oral gavage. After 210 minutes, vehicle (saline) or morphine (2.49 mg/kg) were administered by subcutaneous injection. After an additional 30 min (240 min after ABD-1970 and 30 min after morphine) formalin was administered into the hindpaw and paw licking behavior was monitored using the Laboras™ behavior tracking system.

Complete Freund's Adjuvant (CFA) model of inflammatory pain: male Sprague Dawley rats (200 – 230 g, Charles River Laboratories, Beijing, China) were administered an intraplantar injection of CFA (50 μL, 4 mg/mL) into the dorsal surface of the left hindpaw to induce inflammation and pain (Pharmaron, China). Twenty-four hours after CFA injection, animals were administered vehicle (0.5% methylcellulose) or ABD-1970 (1, 3 and 10 mg/kg) by oral gavage.

Mechanical allodynia in the CFA-injected paw was measured prior to CFA injection and 0 (24 h after CFA and before vehicle or ABD-1970), 2, 4 and 6 h after compound administration by determining withdrawal thresholds to an electronic von Frey instrument (Bioseb, France) applied perpendicularly with increasing force to the plantar surface of the paw. The threshold for paw withdrawal was calculated by taking the average of 2-3 repeated von Frey applications. Observers were blinded to the identity of the treatment groups.

Plantar incision model of post-operative pain: post-operative pain was induced in male Sprague Dawley rats (220 – 250 g, Charles River Laboratories, Beijing, China) as described previously (Brennan et al., 1996) (Pharmaron, China). Briefly, rats were anesthetized with isoflurane, placed in a dorsal recumbent position, and the plantar surface of the left hind foot draped and prepared aseptically. On the plantar surface of the foot, a 1 cm incision was made at 0.5 cm from the edge of the heel and extending distally through the skin and fascia. The plantaris muscle was exposed by blunt dissection, elevated and incised longitudinally, and the skin closed with 2 interrupted mattress sutures (3-0, polydioxanone).

Animals were administered vehicle (0.5% methylcellulose) or ABD-1970 (20 mg/kg) by oral gavage 60 min before anesthesia induction and plantar incision. Buprenorphine (0.03 mg/kg) was administered by intraperitoneal injection immediately before the procedure. Mechanical

JPET Fast Forward. Published on October 10, 2018 as DOI: 10.1124/jpet.118.252296
This article has not been copyedited and formatted. The final version may differ from this version.

allodynia in the operated paw was measured before compound administration (t = 0) to establish pre-surgical baseline withdrawal thresholds, and at 1, 3, and 5 hours after incision using an electronic von Frey instrument (Bioseb, France). Observers were blinded to the identity of the treatment groups.

Chronic constriction injury (CCI) model of peripheral neuropathic pain: CCI on the left common sciatic nerve was performed in male Sprague Dawley rats (Harlan, UK) to induce neuropathic pain as described previously (Bennett and Xie, 1988) (Aquila BioMedical Ltd., UK). Following recovery from anesthesia, animals were recovered for 7 days before behavioral testing was initiated.

Mechanical allodynia was assessed in rats by measuring the withdrawal threshold to von Frey filaments of increasing diameter and force. Animals were placed in a cage with a wire mesh bottom and a series of calibrated von Frey filaments [3.84 (0.6 g), 4.17 (1.4 g), 4.56 (3.8 g), 4.93 (7.1 g), 5.18 (12.4 g) and 5.46 (20.5 g)] were applied to the plantar surface of the left hind paw. Each paw was tested six times with von Frey fibers presented consecutively. A minimum of 3 out of 6 withdrawals was considered a positive response. The middle filament (4.56) was applied first and, if a positive response was observed, the next weaker filament was then tested. Conversely, if the rat did not withdraw its paw at least three times, a larger filament would be tested until a 50% (3/6) withdrawal response was observed. Testing continued in this manner until a withdrawal threshold was reached.

Von Frey thresholds were measured prior to CCI on all rats to establish a baseline withdrawal threshold, and after the CCI procedure on day 7 and 14 to monitor the development of mechanical allodynia. Animals with left paw withdrawal thresholds to von Frey fibers ≤ 8 g were

deemed to have developed mechanical allodynia and were included in the study. Allocation to treatment groups was based on each animal's pre-treatment withdrawal threshold measured on day 14.

On day 14 or 15, animals received a single oral gavage dose of vehicle (0.5% methylcellulose), ABD-1970 or pregabalin (10 mL/kg volume) and 240 min later, mechanical allodynia was measured to determine treatment effects. All observers were blinded to the identity of the treatment groups.

Serotonin-induced scratching model of pruritus: The day before the experiment, female Sprague Dawley rats (202 – 278 g, Janvier Labs, France) were shaved on the rostral part of the back and then placed individually into clear cylindrical observation chambers (height = 35 cm, diameter = 19 cm) for at least 60 minutes to habituate them to the testing environment (Porsolt, France). On the day of the experiment, scratching was induced by intradermal injection of serotonin (50 µL, 50 µg/rat) into the rostral part of the rats back.

To test the effects of ABD-1970 on serotonin-induced scratching, animals were administered vehicle (0.5% methylcellulose) or ABD-1970 (1, 2, or 10 mg/kg) by oral gavage (5 mL/kg volume) 240 minutes before serotonin injection. The positive control naltrexone (NAL, 1 mg/kg) or its respective vehicle (0.9% saline) were administered subcutaneously 15 min before serotonin. Scratching bouts were monitored for 30 min after serotonin injection by an observer blinded to the experimental groups. A single scratching bout was defined as one or more rapid movements of the hindpaws to the area around the site of serotonin injection ending with licking or biting of the toes and/or placement of the hindpaw on the floor of the observation chamber.

Locomotor activity: Open field behavior was monitored in male Sprague Dawley rats 240 min after oral administration of ABD-1970 (1 and 10 mg/kg, 0.5% methylcellulose vehicle) or 15 min after subcutaneous administration of the CB agonist WIN 55,212-2 (3 mg/kg, 1% Tween 80 / 99% saline vehicle) at Saretius Ltd., UK. To control for the different administration times and routes, all animals received counter-balanced vehicle administrations 240 min (0.5% methylcellulose, PO) or 15 min (1% Tween 80 / 99% saline, SC) prior to behavior assessment. Locomotor activity, rearing and grooming were monitored for 40 min using the Laboras™ automated behavioral tracking system.

Prostanoid Production in Stimulated Human Blood and Cells

LPS-stimulated whole blood. Normal human blood was obtained from the Normal Blood Donor Service of The Scripps Research Institute (TSRI) and approved by the TSRI IRB. Blood samples from two donors per experiment (one male and one female donor) was prepared by diluting equal parts heparinized whole blood and serum-free Roswell Park Memorial Institute medium (RPMI) (v/v). Diluted samples (4 mL) were treated with ABD-1970 (0.03 – 30 μM), indomethacin (10 μM), rofecoxib (10 μM) or vehicle (DMSO) for 30 min at 37°C in 24-well plates, and then stimulated with 30 ng/mL of lipopolysaccharides (LPS, Enzo Life Sciences E. coli serotype 0111:B4, # 581-012-L002) or vehicle for ~24 h at 37°C. To collect plasma, well contents were transferred to a 15 mL conical tube and centrifuged at 1,500 rpm for 5 min to pellet erythrocytes. The clear supernatant was isolated, transferred to a glass vial and frozen at -80°C prior to LC-MS/MS analysis as described in the Supplemental Methods.

Ionomycin-stimulated whole blood. Blood from one female donor was prepared by diluting equal parts heparinized whole blood and serum-free RPMI (v/v). Diluted samples (1 mL) were treated

with ABD-1970 (0.3 and 3 μM), indomethacin (10 μM), rofecoxib (10 μM) or vehicle (DMSO) for 30 min at 37°C in 24-well plates, and then stimulated with 30 μM of the calcium ionophore ionomycin (Calbiochem) or vehicle for 30 min at 37°C. To collect plasma, plates were centrifuged at 1,500 rpm for 5 min to pellet erythrocytes. The clear supernatant was isolated, transferred to a glass vial and frozen at -80°C prior to LC-MS/MS analysis as described in the Supplemental Methods.

IL-1β stimulated HUVEC. Primary human umbilical vein endothelial cells (HUVEC) pooled from multiple donors were obtained from Gibco (#C-015-10c, lot #1150190, mycoplasma negative) and expanded in Medium 200 (Gibco #R-001-100) containing low serum growth supplement (Gibco #S-003-10). Cells were plated in 6-well culture dishes ($1x10^6$ million cells per well) until well attached (6 h), washed twice with phenol- and serum-free Medium 200PRF (Gibco, #M-200PRF-500), and then pre-treated for 30 min at 37 °C in 95% O_2 and 5% CO_2 in Medium 200PRF containing one of the following: ABD-1970 (0.1, 10 or 100 nM), indomethacin (500 nM), rofecoxib (500 nM), or DMSO vehicle. Cells were stimulated with IL-1β (1 ng/ml, R&D, #201-LB-005) for ~18 h at 37 °C in 95% O_2 and 5% CO_2. Media was collected, centrifuged to remove non-adherent cells, and frozen at -80°C prior to LC-MS/MS analysis as described in the Supplemental Methods. HUVEC were collected by scraping in cold PBS and frozen at -80°C for subsequent ABPP analysis with FP-Rh to confirm MGLL target engagement and inhibitor selectivity.

Platelet aggregation. The effects of ABD-1970 on platelet aggregation induced by collagen were evaluated essentially as previously described (Born, 1962) (Eurofins Panlabs, Taiwan). Human 60.0 ± 10 kg platelet-rich plasma (6-7 x 10^8 platelets/mL) was treated with 0.3, 3 or 30

μM ABD-1970 or 3 μM indomethacin for 5 minutes at 37°C. Collagen (10 μg/mL) was added to induce aggregation, which was measured by an optical aggregometer.

Statistics

Results are presented as the mean ± standard error of the mean (SEM). Treatment effects on formalin-induced paw licking were analyzed by one-way analysis of variance (ANOVA) followed by Dunnet's post-test or Newman-Keuls multiple comparison tests, as warranted. The CCI study where the effect of treatment on von Frey thresholds versus pre-treatment thresholds were compared was analyzed by a paired Wilcoxon test. Treatment effects on all additional data sets were analyzed by ANOVA and Dunnett's post-test. Differences were considered statistically significant at $p < 0.05$. All statistical analyses were carried out using Prism (version 6; GraphPad Software, La Jolla, CA), SPSS (version 17.0; IBM, Armonk, NY) or Statistica (version 10.1; Statsoft, Palo Alto, CA).

RESULTS

ABD-1970 is a potent and selective inhibitor of MGLL across species.

ABD-1970 (Figure 1) is a member of the carbamate class of MGLL inhibitors, which have been shown to act via covalent carbamylation of the active site serine residue (Butler et al., 2017; Chang et al., 2012; Griebel et al., 2015; Long et al., 2009a; Niphakis et al., 2012). Characterization of ABD-1970 potency and selectivity leveraged ABPP, a chemical proteomics platform that utilizes active-site directed chemical probes to evaluate the activity of entire enzyme families in parallel in native biological matrices (Simon and Cravatt, 2010). *In vitro* treatment of tissue or cell homogenates with ABD-1970, followed by incubation with ABPP

probes, SDS-PAGE analysis and in-gel fluorescence imaging, allows for the direct visualization of the targets of ABD-1970. In this gel-based ABPP platform, quantification of serine hydrolase activity is based on the intensity of probe labeling, and inhibition is measured as a reduction of probe labeling compared to control samples.

ABD-1970 (0.001-10 μM, 30 min, 37°C) was analyzed by ABPP in brain tissue homogenates from mouse, rat, rabbit, dog, monkey and human, as well as in lysates prepared from PC3 cells. Brain tissue was chosen for profiling because it represents an important therapeutic target organ and exhibits high activity of many serine hydrolases, including MGLL. PC3 cells are a rich source of human MGLL, as well as of ABHD6, an off-target common to published MGLL inhibitors (Butler et al., 2017; Chang et al., 2012; Griebel et al., 2015; Long et al., 2009a; Niphakis et al., 2012). Inhibition of MGLL activity was observed following pretreatment with ABD-1970 in brain tissue homogenates of all species and PC3 cell lysates, with average IC_{50} values of < 20 nM (average values presented in Table 1 and representative ABPP gel images and MGLL activity quantitation in Figure 2). MGLL migrates as multiple bands in the ABPP gels, and each band was equally sensitive to ABD-1970. ABD-1970 showed excellent selectivity in all species tested, cross-reacting with only a single off-target, ABHD6, in mouse, rat, rabbit, dog and monkey brain homogenates with IC_{50} values of 3.2, 0.8, 0.6, 1.4, and 3 μM, respectively. ABHD6 was inhibited in human PC3 cells with an IC_{50} of 2.5 μM, while ABHD6 activity was not detected by gel-based ABPP in human brain tissue. Notably, at the concentrations tested, ABD-1970 did not inhibit fatty acid amide hydrolase (FAAH). Since the carbamate functional group of ABD-1970 could be subject to hydrolysis, we evaluated the activity of the amine analog ABD-0038 (Supplemental Figure 1A) using ABPP. Demonstrating that the HFIP carbamate functional group is required for the activity of ABD-1970, ABD-0038

did not inhibit MGLL or other serine hydrolases in mouse, rat and human brain tissue (Supplemental Figure 1B-D).

The cellular activity of ABD-1970 was evaluated in two human systems: cultured PC3 cells and PBMC isolated from human whole blood. When added to the cell culture media, ABD-1970 (0.001-10 μM, 30 min, 37°C) was a potent inhibitor of MGLL in intact PC3 cells, displaying an IC_{50} value of 3.2 nM. MGLL was also inhibited in human PBMC following treatment of whole blood with ABD-1970 (0.03-30 μM, 30 min, 37°C). In this human blood assay, which provides a basis for a clinical peripheral biomarker assay, ABD-1970 treatment inhibited MGLL with an average IC_{50} value of 62 nM (Supplemental Figure 2A).

In order to amplify endocannabinoid signaling and modulate neurotransmission clinically, a MGLL inhibitor must effectively prevent the breakdown of 2-AG in the human nervous system. MGLL has been previously shown to be the major 2-AG hydrolase in the rodent brain both *in vitro* and *in vivo* (Blankman et al., 2007; Long et al., 2009a). Here, we used ABD-1970 to evaluate the contribution of MGLL to 2-AG catabolism in human brain tissue. Inhibition of 2-AG hydrolysis by ABD-1970 (0.0003-1 μM, 30 min, 37°C) was assessed using a MS-based 2-AG substrate assay, which revealed that ~95% of the 2-AG hydrolytic activity in the particulate fraction of human brain cortex was blocked by ABD-1970 with an IC_{50} of 3 nM (Supplemental Figure 2B).

Some carbamate/urea inhibitors of serine hydrolases can display slow reversibility, presumably due to hydrolytic turnover of the carbamylated active site serine residue (Bar-On et al., 2002; Keith et al., 2015). We therefore evaluated the persistence of the ABD-1970-MGLL interaction *in vitro* by assessing enzyme activity over a 24-hour period after removal of excess

compound. Following treatment with ABD-1970 (1 μM, 30 min, 37°C), human MGLL in transfected HEK293T cell lysates remained inhibited by greater than 95% for up to 24 hours after removal of free compound (Supplemental Figure 2C). Based on these measurements, we conclude that the presumed carbamylated adduct formed between hMGLL and ABD-1970 is highly stable over a 24-hour time period, with very little hydrolysis and reactivation of the enzyme.

Considering that ABD-1970 is an irreversible inhibitor of MGLL, we determined a second order rate constant, or k_{inact}/K_i, value for the compound, which provides a measurement of potency that is independent of substrate concentration and pre-incubation time. Using a fluorescent substrate assay, ABD-1970 displayed time-dependent inhibition of purified recombinant human MGLL (Supplemental Figure 2D). The progress curves were fit to a first-order exponential to determine the observed first-order rate constant for enzyme inactivation (k_{obs}) at each concentration of ABD-1970 (Supplemental Figure 2E). Non-linear curve fitting of the k_{obs} versus ABD-1970 concentration plot allowed determination of k_{inact}, K_i and the second-order rate constant k_{inact}/K_i. ABD-1970 displayed an average k_{inact} value of 0.006 s^{-1}, an average K_i value of 0.3 μM, and an average k_{inact}/K_i value of approximately 19,000 $M^{-1}s^{-1}$ against human MGLL.

For irreversible enzyme inhibitors, the recovery of enzymatic activity *in vivo* and in intact cells is largely mediated by protein biosynthesis. To approximate the rate of recovery of MGLL activity following irreversible inhibition in human cells, we measured MGLL activity in cultured PC3 cells for up to 72 hours following incubation with ABD-1970 (10 nM, 30 min, 37°C) and removal of excess compound. ABD-1970 treatment inhibited MGLL activity by approximately

JPET Fast Forward. Published on October 10, 2018 as DOI: 10.1124/jpet.118.252296
This article has not been copyedited and formatted. The final version may differ from this version.

90% at 30 minutes post-treatment, and near-complete recovery of MGLL activity was observed 72 h after free ABD-1970 was removed from the culture media (Supplemental Figure 2F). The average recovery rate for MGLL activity over the course of the experiment (0.5-72 h) was approximately 1% activity per hour.

ABD-1970 is highly selective for MGLL in human tissues and cells.

A comprehensive characterization of the selectivity of ABD-1970 across the serine hydrolase class was performed in human tissues and cells using both gel-based and MS-based ABPP methods. In vitro treatment of human brain (prefrontal cortex), liver, kidney, skin and lung homogenates, or PBMC lysates with ABD-1970 (10 μM, 30 min, 37°C) revealed selective inhibition of MGLL by gel-based ABPP with the FP-Rh probe (Figure 3A). The only off-target of ABD-1970 observed in these tissues was the xenobiotic metabolizing enzyme carboxylesterase 1 (CES1).

The same principles of ABPP can be applied to high-content MS-based proteomic platforms for identification and quantification of protein targets of inhibitors. Here, human brain homogenates were treated with ABD-1970 (0.01-10 μM) or DMSO vehicle for 30 min at 37°C and subjected to MS-based ABPP using the FP-biotin probe to enrich active, but not inhibited serine hydrolases via streptavidin-affinity chromatography (Jessani et al., 2005). Isotopic labels were incorporated into peptides from DMSO- and inhibitor-treated samples, permitting accurate quantitation of relative enzyme activities in a single MS experiment (Boersema et al., 2009). This analysis resulted in the identification and quantification of 78 cerebral human serine hydrolases. Consistent with the gel-based analyses, MGLL was completely inhibited by ABD-1970 at concentrations as low as 0.1 μM, and no off-targets were observed until 10 μM ABD-

1970, at which concentration, ABHD6, CES1 and platelet-activating factor acetylhydrolase (PLA2G7) were also inhibited (Figure 3B). ABD-1970 displays a mean IC_{50} of 0.013 μM towards MGLL in human brain homogenates (Table 1), and therefore, exhibits at least a 77-fold selectivity for MGLL against ABHD6, CES1 and PLA2G7, and at least a 770-fold selectivity for MGLL versus the other 74 enzymes profiled.

ABD-1970 selectively inhibits MGLL in vivo and modulates brain levels of 2-AG, AA and prostanoids.

The dose- and time-dependent effects of oral ABD-1970 administration were evaluated in both mice and rats. Single oral gavage (PO) doses of ABD-1970 (0.1-10 mg/kg) to rats inhibited MGLL in the brain with a median efficacious dose (ED_{50}) of 0.7 mg/kg at 4 hours post-dose (Figure 4A, B). ABD-1970 administration was selective for MGLL amongst rat brain serine hydrolases with only one additional target identified, ABHD6, which was partially inhibited at the highest dose tested of 10 mg/kg (Figure 4A). Significant increases in brain 2-AG concentrations were observed at a dose of 1 mg/kg ABD-1970, near the ED_{50}, with >100 nmol/g 2-AG observed following single doses of 2 or 10 mg/kg (Figure 4C). As has been previously reported in mice treated with MGLL inhibitors (Nomura et al., 2011), reductions in brain AA and the prostanoids PGE_2/D_2 were observed following ABD-1970 administration (Figure 4D). Rat brain concentrations of the other major endocannabinoid anandamide were not affected (Figure 4E).

The time course effects of ABD-1970 were determined in rats following a single oral dose of 12 mg/kg. Exposure to ABD-1970 in brain and blood (Figure 4F) was associated with MGLL inhibition in the brain (Figure 4G) and increases in brain 2-AG concentrations (Figure

4H) for up to 12 hours post-dose. Partial recovery of MGLL activity and normalization of brain 2-AG concentrations were observed by 24 hours post dose.

Similar dose- and time-dependent inhibition of MGLL and accumulation of 2-AG were observed following single oral doses of ABD-1970 in mice (Supplemental Figure 3).

Efficacy of ABD-1970 in the rat formalin model of acute pain correlates with PK and CNS biomarkers and potentiates analgesic standards of care.

MGLL inhibitors produce anti-hyperalgesic and anti-allodynic effects in multiple rodent models of pain (Grabner et al., 2017). To understand the relationship between brain and blood ABD-1970 concentrations, brain MGLL target engagement, brain 2-AG concentrations and antinociceptive efficacy, a pharmacokinetic/pharmacodynamic (PK/PD) relationship was described in the rat formalin model (Tjolsen et al., 1992). Formalin administration to the rat hind paw results in spontaneous pain behaviors, including paw licking, which was quantified using automated behavior tracking cages. Single oral doses of ABD-1970 produced robust antinociceptive activity in formalin-challenged rats (Figure 5A) with an ED_{50} of 1 mg/kg calculated for late phase (10-30 minutes post-formalin) paw licking duration. The reductions in late phase pain behavior at the ED_{50} were associated with ABD-1970 concentrations of 4 nM in the blood and 7 nM in the brain (Figure 5B), 40% inhibition of MGLL in the brain (Figure 5C), and 3-fold increases in brain 2-AG concentrations (Figure 5D).

MGLL inhibitors have been shown to enhance the antinociceptive effects of analgesic drugs in preclinical models of pain (Crowe et al., 2015; Crowe et al., 2017; Wilkerson et al., 2016). We evaluated the effects of ABD-1970 in combination with the alpha-2, delta-1 calcium

channel blocker preabalin or the mu opioid receptor agonist morphine in the rat formalin model. Co-administration of ABD-1970 and pregabalin significantly reduced paw licking pain behavior in formalin-treated rats to a greater extent than either agent individually (Figure 5E). Treatment of rats with ABD-1970 and morphine similarly reduced formalin responses, while administration of either compound alone lacked efficacy in this experiment (Figure 5F). These results demonstrate that MGLL inhibition potentiates the antinociceptive effects of mechanistically distinct and clinically effective analgesics.

ABD-1970 demonstrates broad-spectrum antinociceptive and anti-pruritic effects without cannabimimetic effects on locomotor activity.

ABD-1970 was tested in additional preclinical models of pain of distinct pathologic origins and in a model of pruritis. In the inflammatory pain model caused by plantar injection of Complete Freund's Adjuvant (CFA), ABD-1970 administration produced dose-dependent anti-allodynic effects for up to 6 hours post-dose, with a calculated ED_{50} value of 2 mg/kg at 4 hours post-dose (Figure 6A). A single dose of 20 mg/kg ABD-1970 reduced mechanical allodynia in rats caused by plantar incision to a similar extent as a non-sedative dose of the opioid buprenorphine (Figure 6B). In the CCI model of neuropathic pain, a single dose of 30 mg/kg ABD-1970 or pregabalin significantly reversed allodynic responses compared to vehicle treated rats (Figure 6C). In a rat model of pruritus induced by intradermal injection of serotonin, ABD-1970 demonstrated significant anti-pruritic effects at doses as low at 1 mg/kg that were similar to that of the opioid antagonist naltrexone (Figure 6D).

The antinociceptive and anti-pruritic effects observed following ABD-1970 treatment occurred without overt behavioral effects. Single doses of 1 and 10 mg/kg of ABD-1970 did not

reduce locomotor duration in a novel environment (Figure 6E) or rearing (Figure 6F), but did produce dose-dependent reductions in grooming (Figure 6G). In stark contrast, a single 3 mg/kg dose of the exogenous cannabinoid WIN 55,212-2 dramatically reduced locomotor activity, rearing and grooming (Figure 6E-G).

MGLL and COX inhibition differentially affect prostanoid production in human cells

The anatomically contextualized contribution of MGLL to prostanoid metabolism in mice (Nomura et al., 2011) motivated us to evaluate the effects of ABD-1970 in human cellular systems alongside the nonselective COX inhibitor, indomethacin, and selective COX2 inhibitor, rofecoxib. Human whole blood can be stimulated with lipopolysaccharide (LPS) endotoxin or calcium ionophores to produce inflammatory prostanoids, which are strongly suppressed by COX inhibition (Brideau et al., 1996; Warner et al., 1999). ABD-1970 treatment of whole blood effectively inhibits MGLL activity in PBMC (IC_{50} = 62 nM). Therefore, human blood represents an appropriate system to evaluate the effects of MGLL inhibition on stimulated prostanoid production and compare them with the effects of COX inhibition.

Human whole blood from two donors was treated with LPS (30 ng/mL, 37°C, ~24 h) to stimulate prostanoid production. Pretreatment of LPS-stimulated whole blood with ABD-1970 (0.03-30 μM, 30 min, 37°C) increased plasma 2-AG by ~7-fold (Figure 7A), and decreased plasma AA by ~2-fold (Figure 7B), but did not affect prostaglandin E2 (PGE_2) or TXB_2 concentrations (Figure 7C). In contrast, pretreatment of whole blood with the NSAID indomethacin (30 μM, 30 min, 37°C) suppressed production of PGE_2 and TXB_2 by more than 10-fold. The selective COX2 inhibitor rofecoxib (10 μM, 30 min, 37°C) also suppressed PGE_2,

JPET Fast Forward. Published on October 10, 2018 as DOI: 10.1124/jpet.118.252296
This article has not been copyedited and formatted. The final version may differ from this version.

and to a lesser degree, TXB_2, consistent with the dominant role of COX1 in thromboxane production in blood (Brideau et al., 1996; Warner et al., 1999).

Stimulation of human whole blood with the calcium ionophore ionomycin (30 μM, 30 min, 37°C) increased production of AA (Figure 7D), and prostanoids (PGE_2 and TXB_2) (Figure 6E), as expected. Pretreatment of ionomycin-stimulated whole blood with ABD-1970 (0.3 and 3 μM) did not significantly alter plasma levels of AA (Figure 7D) or of downstream prostanoid lipids (Figure 7E). In contrast, indomethacin (10 μM, 30 min, 37°C) suppressed production of PGE_2 and TXB_2 by 10-fold or greater (Figure 7E), while rofecoxib (10 μM, 30 min, 37°C) suppressed both PGE_2 and TXB_2 by ~3-fold (Figure 7E).

The impact of MGLL inhibition on prostanoid production in human endothelial cells was investigated in primary HUVEC stimulated with the inflammatory cytokine interleukin-1 beta (IL-1β). HUVEC have previously been used to study the effect of COX inhibition on prostanoid production, as they generate important signaling active prostanoid lipids when stimulated (Niederberger et al., 2004; Salvado et al., 2009). These lipids include thromboxane A_2 (measured as its stable breakdown product TXB_2), which stimulates platelet aggregation and vasoconstriction, and prostacyclin (measured as its stable breakdown product 6-ketoprostaglandin F1α (6k-$PGF_{1\alpha}$), which inhibits platelet aggregation and causes vasodilation (Salvado et al., 2009).

Stimulation of HUVEC with IL-1β increased the production of several prostanoid lipids including 6k-$PGF_{1\alpha}$, TXB_2, and Prostaglandin F2α ($PGF_{2\alpha}$) (Figure 7F). All of these prostanoids were suppressed when pre-stimulated HUVEC were treated with indomethacin (500 nM) or

rofecoxib (500 nM), but not ABD-1970 (0.1-100 nM), despite confirmation of complete MGLL inhibition at 10 and 100 nM ABD-1970 (Supplemental Figure 4).

To investigate the functional consequences of MGLL inhibition on prostanoid signaling, ABD-1970 was tested for its effect on collagen-induced platelet aggregation, an assay in which NSAIDs display robust anti-aggregatory activity (Armstrong et al., 2008). In human platelet-rich plasma, ABD-1970 (0.3-30 μM) did not promote platelet aggregation or suppress aggregation induced by collagen (0% agonist or antagonist activity at 0.3, 3 and 30 μM ABD-1970). In contrast, indomethacin (3 μM) suppressed collagen-induced aggregation by 98%.

DISCUSSION

Preparations of *Cannabis* and cannabinoid receptor agonists produce therapeutic effects in man, which are accompanied by adverse CNS effects that limit the clinical dose. An alternative strategy to harness the clinical utility of cannabinoid receptor activation is to augment endocannabinoid signaling by limiting enzymatic degradation. MGLL is the major 2-AG hydrolase in rodents, and MGLL inhibitors produce a myriad of beneficial effects in animal models of pain, anxiety, epilepsy, traumatic brain injury, neuroinflammation and neurodegeneration (Chen et al., 2012; Grabner et al., 2017; Griebel et al., 2015; Katz et al., 2015; Nomura et al., 2011; Patel et al., 2017; Piro et al., 2012; Sugaya et al., 2016; von Ruden et al., 2015; Zhang et al., 2015). To prepare for a MGLL inhibitor clinical program, we developed the selective MGLL inhibitor tool compound ABD-1970 to evaluate the consequences of MGLL inhibition in human tissues and cells, and in rodent models of pain and pruritus.

ABD-1970 is a potent inhibitor of MGLL across species that acts via a time-dependent and irreversible mechanism, which is consistent with a covalent interaction, as has been observed for other mechanism-based carbamate-containing MGLL inhibitors (Butler et al., 2017; Chang et al., 2012; Griebel et al., 2015; Long et al., 2009a; Niphakis et al., 2012). Covalent inhibition can be an attractive mechanism for enzyme inactivation as high biochemical efficiency and extended duration of target engagement, compared to the pharmacokinetic profile, can often be achieved (Johnson et al., 2010; Singh et al., 2011). The time-dependent and irreversible nature of the ABD-1970-MGLL interaction likely contributes to the high potency and sustained activity that ABD-1970 displays in vivo. Once MGLL is inhibited, ABD-1970 does not need to compete with rising 2-AG concentrations, which ultimately reach > 100 nanomoles per gram (~ 100 μM) in the brain, and the maintenance of inhibition is not solely determined by sustained compound exposure, but instead, is largely dependent on protein biosynthesis.

The exceptional potency and selectivity of ABD-1970 was achieved through a medicinal chemistry campaign that leveraged the chemical proteomics platform ABPP (Niphakis and Cravatt, 2014) to simultaneously evaluate and optimize these parameters (Cisar et al., 2018). Extensive ABPP profiling in human tissues and cells revealed that ABD-1970 has at least a 77-fold selectivity towards MGLL over other serine hydrolases and completely inhibits MGLL at concentrations that are devoid of any serine hydrolase off-target interactions. Of the >70 serine hydrolase enzymes screened, many are wholly uncharacterized with regards to their substrates and functions, and, as such, substrate-agnostic techniques like ABPP represent the only way to functionally evaluate these enzymes and confirm selectivity.

The favorable pharmacological profile demonstrated by ABD-1970 in vitro was maintained in vivo following oral administration to mice and rats, as ABD-1970 selectively and sustainably inhibited MGLL in the brain with concomitant increases in whole brain 2-AG concentrations. Single doses of ABD-1970 effectively inhibited brain MGLL activity in both species with ED_{50} values of approximately 1 mg/kg. The dose-response relationship revealed marked sensitivity of brain 2-AG to MGLL activity as partial inhibition of MGLL in the brain was sufficient to elevate 2-AG levels, which ultimately increased by >10-fold once MGLL was completely inhibited. In contrast, in the rat, ~2-fold reductions in levels of AA and the prostaglandins PGE_2/D_2 in the brain were associated with near complete inhibition of MGLL.

To understand the relationship between ABD-1970 PK, MGLL target engagement, 2-AG, and antinociceptive efficacy, we used the rat formalin pain model. This model provided the opportunity to evaluate the effects of ABD-1970 administration on two distinct nociceptive modalities: an early phase corresponding to direct activation of peripheral sensory nerves and a late phase corresponding largely to central sensitization (Tjolsen et al., 1992). Single doses of ABD-1970 numerically reduced pain behavior in the early phase and significantly reduced pain behaviors in the late phase of the formalin response with and ED_{50} of 1 mg/kg. The antinociceptive effects observed at the ED_{50} were associated with ABD-1970 concentrations less than 10 nM in the brain and blood, 40% inhibition of brain MGLL activity and 3-fold elevations in brain 2-AG concentrations. Multiple previous studies have demonstrated sustained antinociceptive, antiallodynic and antihyperalgesic effects following repeated administration of MGLL inhibitors at low doses that partially inhibit MGLL in the brain (Burston et al., 2016; Busquets-Garcia et al., 2011; Curry et al., 2018; Kinsey et al., 2013), whereas tolerance to these effects has been observed following prolonged, complete MGLL inhibition or genetic ablation

(Chanda et al., 2010; Ignatowska-Jankowska et al., 2014; Schlosburg et al., 2010). The functional tolerance observed with complete MGLL inactivation and maximal elevation of brain 2-AG concentrations is associated with down regulation and/or desensitization of brain CB_1 receptors (Chanda et al., 2010; Navia-Paldanius et al., 2015; Schlosburg et al., 2010). The ABD-1970 PK/PD relationship in the rat formalin model revealed that pain-modifying activity was observed at low doses and exposures of ABD-1970 that only partially inhibited brain MGLL and caused sub-maximal elevations of 2-AG in the brain. Therefore, low doses of ABD-1970 near the ED_{50} of 1 mg/kg would be predicted to maintain efficacy following repeated dosing.

In addition to demonstrating significant antinociceptive activity as a single agent in the rat formalin model, ABD-1970 also potentiated the activity of two analgesic standards of care: pregabalin and morphine, in agreement with the synergistic activity that has been previously shown for MGLL inhibitors and similar agents in other pain models (Crowe et al., 2017; Wilkerson et al., 2016). That MGLL inhibition enhanced the efficacy of these clinically effective drugs, suggests that in addition to providing pain relief as a single agent, a MGLL inhibitor may find clinical utility in enhancing the effectiveness of non-narcotic pain killers like pregabalin or limiting the dose needed of opioid drugs to provide adequate pain relief. The effects of ABD-1970 on pain were not limited to acute pain caused by formalin; antinociceptive or anti-allodynic effects were observed in rat models of post-operative pain, neuropathic pain and inflammatory pain. ABD-1970 also significantly reduced itch behavior in the rat serotonin model of pruritis, consistent with previously published reports with MGLL inhibitors in mice (Tosun et al., 2015; Yesilyurt et al., 2016). These effects occurred without obvious cannabimimetic effects or sedation as ABD-1970 did not reproduce the behavioral effects of the direct cannabinoid receptor agonist WIN 55,212-2 in a novel open field. ABD-1970 did dose-dependently reduce

grooming behavior in the novel environment, which may be related to the anti-pruritic and anxiolytic effects of this mechanism.

Selective MGLL inhibition by ABD-1970 in the rodent brain effectively increased total brain 2-AG concentrations, as has been previously demonstrated following pharmacological or genetic inactivation of MGLL (Long et al., 2009a; Schlosburg et al., 2010). Experiments with ABD-1970 in human tissues and cells suggest that MGLL is likely to similarly regulate 2-AG in man. ABD-1970 treatment of human brain tissue reduced 2-AG hydrolysis by >95%, which is comparable to the ~85% of the total 2-AG hydrolase activity mediated by MGLL in mouse brain preparations (Blankman et al., 2007), therefore increasing confidence that MGLL inhibition in the human brain will amplify 2-AG signaling and produce the therapeutically beneficial effects demonstrated in preclinical studies. Likewise, treatment of human whole blood with ABD-1970 inhibited MGLL in blood cells and elevated plasma 2-AG concentrations. The concentration-dependent inhibition of MGLL observed in PBMC following treatment of whole blood provides a viable clinical biomarker strategy to measure peripheral MGLL target engagement in human subjects or patients administered a MGLL inhibitor.

In rodents, MGLL serves as a source of AA for COX-mediated prostanoid generation in in a subset of tissues (Nomura et al., 2011). Here, we used ABD-1970 to evaluate the contribution of MGLL to the generation of AA-derived prostanoids in human whole blood and endothelial cells. The non-selective COX inhibitor indomethacin and selective COX2 inhibitor rofecoxib were evaluated in parallel to compare the effects of MGLL and COX inhibition in assays known to be sensitive to COX inhibitors. MGLL inhibition did not suppress stimulated prostanoid production or platelet aggregation and was therefore differentiated from COX

inhibition. Our results show that despite their involvement in sequential steps of the arachidonic acid metabolic pathway, the effects of inhibiting MGLL or COX enzymes in human cells are distinct, suggesting that MGLL inhibitors are unlikely to replicate the toxicity profiles displayed by COX inhibitors.

In conclusion, ABD-1970 is a highly potent, selective and orally bioavailable MGLL inhibitor, which we have used to evaluate the effects of MGLL inhibition in human tissues and cells and rodent models of pain and itch. These results support use of ABD-1970 as a tool MGLL inhibitor in preclinical models and further clinical exploration of the mechanism. Towards this end, we have developed a mechanistically similar MGLL inhibitor that is currently in clinical development for neurological indications, including Tourette syndrome, spasticity in multiple sclerosis, and pain (Cisar et al., 2018).

ACKNOWLEDGMENTS

We would like to thank Dr. Guy Kennett of Saretius for helpful discussions and insight into the formalin pain model and Drs. Clare Doris and Hayley Gooding at Aquila BioMedical and Dr. Jenny Wilkerson and Professor Aron Lichtman at Virginia Commonwealth University assistance with the chronic constriction injury model. We thank Dr. Nathalie C. Franc (Franc consulting, San Diego, CA) for providing medical writing support (editing and formatting). We thank Professor Ben Cravatt at The Scripps Research Institute for critical reading of the manuscript.

AUTHORSHIP CONTRIBUTIONS

Authorship Responsibility:

Participated in research design: Clapper, Fraser, Ezekowitz, O'Neill and Blankman; Conducted experiments: Clapper, Henry, Niphakis, Knize, Coppola, Simon, Ngo, R.A. Herbst, D.M. Herbst, Reed, Viader, Alexander, Cunningham and Blankman; Contributed new reagents or analytic tools: Cisar, Weber, Jones and Grice; Performed data analysis: Clapper, Niphakis, Simon, Viader, Alexander, Cunningham and Blankman; Wrote or contributed to the writing of the manuscript: Clapper, Henry, Niphakis, Knize, Cisar, O'Neill and Blankman.

Chemical structure statement: The chemical structure of the compounds ABD-1970 and ABD-0038 discussed here are presented in Figure 1 and Supplemental Figure 1, in accordance with the journal's editorial policy.

REFERENCES

Abbott FV, Franklin KB, and Westbrook RF (1995). The formalin test: scoring properties of the first and second phases of the pain response in rats. Pain *60*, 91-102.

Armstrong PC, Truss NJ, Ali FY, Dhanji AA, Vojnovic I, Zain ZN, Bishop-Bailey D, Paul-Clark MJ, Tucker AT, Mitchell JA, and Warner TD (2008). Aspirin and the in vitro linear relationship between thromboxane A2-mediated platelet aggregation and platelet production of thromboxane A2. J Thromb Haemost *6*, 1933-1943.

Bar-On P, Millard CB, Harel M, Dvir H, Enz A, Sussman JL, and Silman I (2002). Kinetic and structural studies on the interaction of cholinesterases with the anti-Alzheimer drug rivastigmine. Biochem *41*, 3555-3564.

Bedse G, Bluett RJ, Patrick TA, Romness NK, Gaulden AD, Kingsley PJ, Plath N, Marnett LJ, and Patel S (2018). Therapeutic endocannabinoid augmentation for mood and anxiety disorders: comparative profiling of FAAH, MAGL and dual inhibitors. Transl Psychiatry *8*, 92.

Bennett GJ, and Xie YK (1988). A peripheral mononeuropathy in rat that produces disorders of pain sensation like those seen in man. Pain *33*, 87-107.

Berry LM, Wollenberg L, and Zhao Z (2009). Esterase activities in the blood, liver and intestine of several preclinical species and humans. Drug Metab Lett *3*, 70-77.

Blankman JL, Simon GM, and Cravatt BF (2007). A Comprehensive Profile of Brain Enzymes that Hydrolyze the Endocannabinoid 2-Arachidonoylglycerol. Chem Biol *14*, 1347-1356.

Boersema PJ, Raijmakers R, Lemeer S, Mohammed S, and Heck AJ (2009). Multiplex peptide stable isotope dimethyl labeling for quantitative proteomics. Nat Protoc *4*, 484-494.

Born GV (1962). Aggregation of blood platelets by adenosine diphosphate and its reversal. Nature *194*, 927-929.

Brennan TJ, Vandermeulen EP, and Gebhart GF (1996). Characterization of a rat model of incisional pain. Pain *64*, 493-501.

Brideau C, Kargman S, Liu S, Dallob AL, Ehrich EW, Rodger IW, and Chan CC (1996). A human whole blood assay for clinical evaluation of biochemical efficacy of cyclooxygenase inhibitors. Inflamm Res *45*, 68-74.

Burston JJ, Mapp PI, Sarmad S, Barrett DA, Niphakis MJ, Cravatt BF, Walsh DA, and Chapman V (2016). Robust anti-nociceptive effects of monoacylglycerol lipase inhibition in a model of osteoarthritis pain. Br J Pharmacol *173*, 3134-3144.

Busquets-Garcia A, Puighermanal E, Pastor A, de la Torre R, Maldonado R, and Ozaita A (2011). Differential role of anandamide and 2-arachidonoylglycerol in memory and anxiety-like responses. Biol Psychiatry *70*, 479-486.

Butler CR, Beck EM, Harris A, Huang Z, McAllister LA, and Am Ende CW (2017). Azetidine and Piperidine Carbamates as Efficient, Covalent Inhibitors of Monoacylglycerol Lipase. J Med Chem *60*, 9860-9873.

Chanda PK, Gao Y, Mark L, Btesh J, Strassle BW, Lu P, Piesla MJ, Zhang MY, Bingham B, Uveges A, Kowal D, Garbe D, Kouranova EV, Ring RH, Bates B, Pangalos MN, Kennedy JD, Whiteside GT, and Samad TA (2010). Monoacylglycerol lipase activity is a critical modulator of the tone and integrity of the endocannabinoid system. Molecular pharmacology *78*, 996-1003.

Chang JW, Cognetta AB, 3rd, Niphakis MJ, and Cravatt BF (2013). Proteome-wide reactivity profiling identifies diverse carbamate chemotypes tuned for serine hydrolase inhibition. ACS Chem Biol *8*, 1590-1599.

Chang JW, Niphakis MJ, Lum KM, Cognetta AB, 3rd, Wang C, Matthews ML, Niessen S, Buczynski MW, Parsons LH, and Cravatt BF (2012). Highly selective inhibitors of

monoacylglycerol lipase bearing a reactive group that is bioisosteric with endocannabinoid substrates. Chem Biol *19*, 579-588.

Chen R, Zhang J, Wu Y, Wang D, Feng G, Tang Y-P, Teng Z, and Chen C (2012). Monoacylglycerol Lipase Is a Therapeutic Target for Alzheimer's Disease. Cell Rep *2*, 1329-1339.

Cisar JS, Weber OD, Clapper JR, Blankman JL, Henry CL, Simon GM, Alexander JP, Jones TK, Ezekowitz RAB, O'Neill GP, and Grice CA (2018). Identification of ABX-1431, a Selective Inhibitor of Monoacylglycerol Lipase and Clinical Candidate for Treatment of Neurological Disorders. J Med Chem.

Copeland RA (2000). Enzymes: A Practical Introduction to Structure, Mechanism, and Data Analysis, Second Edition edn (New York: Wiley-VCH).

Crowe MS, and Kinsey SG (2017). MAGL inhibition modulates gastric secretion and motility following NSAID exposure in mice. Eur J Pharmacol *807*, 198-204.

Crowe MS, Leishman E, Banks ML, Gujjar R, Mahadevan A, Bradshaw HB, and Kinsey SG (2015). Combined inhibition of monoacylglycerol lipase and cyclooxygenases synergistically reduces neuropathic pain in mice. Br J Pharmacol *172*, 1700-1712.

Crowe MS, Wilson CD, Leishman E, Prather PL, Bradshaw HB, and Banks ML (2017). The monoacylglycerol lipase inhibitor KML29 with gabapentin synergistically produces analgesia in mice. Br J Pharmacol *174*, 4523-4539.

Curry ZA, Wilkerson JL, Bagdas D, Kyte SL, Patel N, Donvito G, Mustafa MA, Poklis JL, Niphakis MJ, Hsu KL, Cravatt BF, Gewirtz DA, Damaj MI, and Lichtman AH (2018). Monoacylglycerol Lipase Inhibitors Reverse Paclitaxel-Induced Nociceptive Behavior and Proinflammatory Markers in a Mouse Model of Chemotherapy-Induced Neuropathy. J Pharmacol Exp Ther *366*, 169-183.

Funk CD (2001). Prostaglandins and leukotrienes: advances in eicosanoid biology. Science *294*, 1871-1875.

Grabner GF, Zimmermann R, Schicho R, and Taschler U (2017). Monoglyceride lipase as a drug target: At the crossroads of arachidonic acid metabolism and endocannabinoid signaling. Pharmacol Ther *175*, 35-46.

Griebel G, Pichat P, Beeske S, Leroy T, Redon N, Jacquet A, Francon D, Bert L, Even L, Lopez-Grancha M, Tolstykh T, Sun F, Yu Q, Brittain S, Arlt H, He T, Zhang B, Wiederschain D, Bertrand T, Houtmann J, Rak A, Vallee F, Michot N, Auge F, Menet V, Bergis OE, George P, Avenet P, Mikol V, Didier M, and Escoubet J (2015). Selective blockade of the hydrolysis of the endocannabinoid 2-arachidonoylglycerol impairs learning and memory performance while producing antinociceptive activity in rodents. Sci Rep *5*, 7642.

Gulyas AI, Cravatt BF, Bracey MH, Dinh TP, Piomelli D, Boscia F, and Freund TF (2004). Segregation of two endocannabinoid-hydrolyzing enzymes into pre- and postsynaptic compartments in the rat hippocampus, cerebellum and amygdala. Eur J Neurosci *20*, 441-458.

Hsu K-L, Tsuboi K, Adibekian A, Pugh H, Masuda K, and Cravatt BF (2012). DAGLβ inhibition perturbs a lipid network involved in macrophage inflammatory responses. Nat Chem Biol *8*, 999-1007.

Ignatowska-Jankowska B, Wilkerson JL, Mustafa M, Abdullah R, Niphakis M, Wiley JL, Cravatt BF, and Lichtman AH (2015). Selective monoacylglycerol lipase inhibitors: antinociceptive versus cannabimimetic effects in mice. J Pharmacol Exp Ther *353*, 424-432.

Ignatowska-Jankowska BM, Ghosh S, Crowe MS, Kinsey SG, Niphakis MJ, Abdullah RA, Tao Q, O' Neal ST, Walentiny DM, Wiley JL, Cravatt BF, and Lichtman AH (2014). In vivo

characterization of the highly selective monoacylglycerol lipase inhibitor KML29: antinociceptive activity without cannabimimetic side effects. Br J Pharmacol *171*, 1392-1407.

Jessani N, Niessen S, Wei BQ, Nicolau M, Humphrey M, Ji Y, Han W, Noh DY, Yates JR, 3rd, Jeffrey SS, and Cravatt BF (2005). A streamlined platform for high-content functional proteomics of primary human specimens. Nat Methods *2*, 691-697.

Johnson DS, Weerapana E, and Cravatt BF (2010). Strategies for discovering and derisking covalent, irreversible enzyme inhibitors. Future Med Chem *2*, 949-964.

Kano M, Ohno-Shosaku T, Hashimotodani Y, Uchigashima M, and Watanabe M (2009). Endocannabinoid-Mediated Control of Synaptic Transmission. Physiol Rev *89*, 309-380.

Katona I, and Freund TF (2008). Endocannabinoid signaling as a synaptic circuit breaker in neurological disease. Nat Med *14*, 923-930.

Katona I, Urban GM, Wallace M, Ledent C, Jung KM, Piomelli D, Mackie K, and Freund TF (2006). Molecular composition of the endocannabinoid system at glutamatergic synapses. J Neurosci *26*, 5628-5637.

Katz PS, Sulzer JK, Impastato RA, Teng SX, Rogers EK, and Molina PE (2015). Endocannabinoid degradation inhibition improves neurobehavioral function, blood-brain barrier integrity, and neuroinflammation following mild traumatic brain injury. J Neurotrauma *32*, 297-306.

Keith JM, Jones WM, Tichenor M, Liu J, Seierstad M, Palmer JA, Webb M, Karbarz M, Scott BP, Wilson SJ, Luo L, Wennerholm ML, Chang L, Rizzolio M, Rynberg R, Chaplan SR, and Breitenbucher JG (2015). Preclinical Characterization of the FAAH Inhibitor JNJ-42165279. ACS Med Chem Lett *6*, 1204-1208.

Kinsey SG, Nomura DK, O'Neal ST, Long JZ, Mahadevan A, Cravatt BF, Grider JR, and Lichtman AH (2011). Inhibition of Monoacylglycerol Lipase Attenuates Nonsteroidal Anti-

Inflammatory Drug-Induced Gastric Hemorrhages in Mice. J Pharmacol Exp Ther *338*, 795-802.

Kinsey SG, Wise LE, Ramesh D, Abdullah R, Selley DE, Cravatt BF, and Lichtman AH (2013). Repeated low-dose administration of the monoacylglycerol lipase inhibitor JZL184 retains cannabinoid receptor type 1-mediated antinociceptive and gastroprotective effects. J Pharmacol Exp Ther *345*, 492-501.

Leung D, Hardouin C, Boger DL, and Cravatt BF (2003). Discovering potent and selective inhibitors of enzymes in complex proteomes. Nat Biotechnol *21*, 687-691.

Long JZ, Li W, Booker L, Burston JJ, Kinsey SG, Schlosburg JE, Pavon FJ, Serrano AM, Selley DE, Parsons LH, Lichtman AH, and Cravatt BF (2009a). Selective blockade of 2-arachidonoylglycerol hydrolysis produces cannabinoid behavioral effects. Nat Chem Biol *5*, 37-44.

Long JZ, Nomura DK, and Cravatt BF (2009b). Characterization of Monoacylglycerol Lipase Inhibition Reveals Differences in Central and Peripheral Endocannabinoid Metabolism. Chem Biol *16*, 744-753.

Mechoulam R, Ben-Shabat S, Hanus L, Ligumsky M, Kaminski NE, Schatz AR, Gopher A, Almog S, Martin BR, and Compton DR (1995). Identification of an endogenous 2-monoglyceride, present in canine gut, that binds cannabinoid receptors. Biochem Pharmacol *50*, 83-90.

Navia-Paldanius D, Aaltonen N, Lehtonen M, Savinainen JR, Taschler U, Radner FP, Zimmermann R, and Laitinen JT (2015). Increased tonic cannabinoid CB1R activity and brain region-specific desensitization of CB1R Gi/o signaling axis in mice with global genetic knockout of monoacylglycerol lipase. Eur J Pharm Sci *77*, 180-188.

Niederberger E, Manderscheid C, Grösch S, Schmidt H, Ehnert C, and Geisslinger G (2004). Effects of the selective COX-2 inhibitors celecoxib and rofecoxib on human vascular cells. Biochem Pharmacol *68*, 341-350.

Niphakis MJ, and Cravatt BF (2014). Enzyme inhibitor discovery by activity-based protein profiling. Annu Rev Biochem *83*, 341-377.

Niphakis MJ, Johnson DS, Ballard ET, Stiff C, and Cravatt BF (2012). O-Hydroxyacetamide Carbamates as a Highly Potent and Selective Class of Endocannabinoid Hydrolase Inhibitors. ACS Chem Neurosci *3*, 418-426.

Nomura DK, Morrison BE, Blankman JL, Long JZ, Kinsey SG, Marcondes MCG, Ward AM, Hahn YK, Lichtman AH, Conti B, and Cravatt BF (2011). Endocannabinoid Hydrolysis Generates Brain Prostaglandins That Promote Neuroinflammation. Science *334*, 809-813.

Patel S, Hill MN, Cheer JF, Wotjak CT, and Holmes A (2017). The endocannabinoid system as a target for novel anxiolytic drugs. Neurosci Biobehav Rev *76*, 56-66.

Patricelli MP, Giang DK, Stamp LM, and Burbaum JJ (2001). Direct visualization of serine hydrolase activities in complex proteome using fluorescent active site-directed probes. Proteomics *1*, 1067-1071.

Pertwee RG (2012). Targeting the endocannabinoid system with cannabinoid receptor agonists: pharmacological strategies and therapeutic possibilities. Philos Trans R Soc Lond B Biol Sci *367*, 3353-3363.

Piro Justin R, Benjamin Daniel I, Duerr James M, Pi Y, Gonzales C, Wood Kathleen M, Schwartz Joel W, Nomura Daniel K, and Samad Tarek A (2012). A Dysregulated Endocannabinoid-Eicosanoid Network Supports Pathogenesis in a Mouse Model of Alzheimer's Disease. Cell Rep *1*, 617-623.

Salvado MD, Alfranca A, Escolano A, Haeggström JZ, and Redondo JM (2009). COX-2 Limits Prostanoid Production in Activated HUVECs and Is a Source of PGH2 for Transcellular Metabolism to PGE2 by Tumor Cells. Arterioscler Thromb and Vasc Biol *29*, 1131-1137.

Schlosburg JE, Blankman JL, Long JZ, Nomura DK, Pan B, Kinsey SG, Nguyen PT, Ramesh D, Booker L, Burston JJ, Thomas EA, Selley DE, Sim-Selley LJ, Liu QS, Lichtman AH, and Cravatt BF (2010). Chronic monoacylglycerol lipase blockade causes functional antagonism of the endocannabinoid system. Nat Neurosci *13*, 1113-1119.

Simon GM, and Cravatt BF (2010). Activity-based Proteomics of Enzyme Superfamilies: Serine Hydrolases as a Case Study. J Biol Chem *285*, 11051-11055.

Singh J, Petter RC, Baillie TA, and Whitty A (2011). The resurgence of covalent drugs. Nat Rev Drug Discov *10*, 307-317.

Sugaya Y, Yamazaki M, Uchigashima M, Kobayashi K, Watanabe M, Sakimura K, and Kano M (2016). Crucial Roles of the Endocannabinoid 2-Arachidonoylglycerol in the Suppression of Epileptic Seizures. Cell Rep *16*, 1405-1415.

Sugiura T, Kondo S, Sukagawa A, Nakane S, Shinoda A, Itoh K, Yamashita A, and Waku K (1995). 2-Arachidonylglycerol: a possible endogenous cannabinoid receptor ligand in brain. Biochem Biophys Res Commun *215*, 89-97.

Terrone G, Pauletti A, Salamone A, Rizzi M, Villa BR, Porcu L, Sheehan MJ, Guilmette E, Butler CR, Piro JR, Samad TA, and Vezzani A (2018). Inhibition of monoacylglycerol lipase terminates diazepam-resistant status epilepticus in mice and its effects are potentiated by a ketogenic diet. Epilepsia *59*, 79-91.

Tjolsen A, Berge OG, Hunskaar S, Rosland JH, and Hole K (1992). The formalin test: an evaluation of the method. Pain *51*, 5-17.

Tosun NC, Gunduz O, and Ulugol A (2015). Attenuation of serotonin-induced itch responses by inhibition of endocannabinoid degradative enzymes, fatty acid amide hydrolase and monoacylglycerol lipase. J Neural Transm (Vienna) *122*, 363-367.

Viader A, Blankman JL, Zhong P, Liu X, Schlosburg JE, Joslyn CM, Liu QS, Tomarchio AJ, Lichtman AH, Selley DE, Sim-Selley LJ, and Cravatt BF (2015). Metabolic Interplay between Astrocytes and Neurons Regulates Endocannabinoid Action. Cell Rep *12*, 798-808.

von Ruden EL, Bogdanovic RM, Wotjak CT, and Potschka H (2015). Inhibition of monoacylglycerol lipase mediates a cannabinoid 1-receptor dependent delay of kindling progression in mice. Neurobiol Dis *77*, 238-245.

Warner TD, Giuliano F, Vojnovic I, Bukasa A, Mitchell JA, and Vane JR (1999). Nonsteroid drug selectivities for cyclo-oxygenase-1 rather than cyclo-oxygenase-2 are associated with human gastrointestinal toxicity: a full in vitro analysis. Proc Natl Acad Sci U S A *96*, 7563-7568.

Wilkerson JL, Niphakis MJ, Grim TW, Mustafa MA, Abdullah RA, Poklis JL, Dewey WL, Akbarali H, Banks ML, Wise LE, Cravatt BF, and Lichtman AH (2016). The Selective Monoacylglycerol Lipase Inhibitor MJN110 Produces Opioid-Sparing Effects in a Mouse Neuropathic Pain Model. J Pharmacol Exp Ther *357*, 145-156.

Yesilyurt O, Cayirli M, Sakin YS, Seyrek M, Akar A, and Dogrul A (2016). Systemic and spinal administration of FAAH, MAGL inhibitors and dual FAAH/MAGL inhibitors produce antipruritic effect in mice. Archives Dermatol Res *308*, 335-345.

Zhang J, and Chen C (2018). Alleviation of Neuropathology by Inhibition of Monoacylglycerol Lipase in APP Transgenic Mice Lacking CB2 Receptors. Mol Neurobiol *Jun;55*, 4802-4810.

Zhang J, Teng Z, Song Y, Hu M, and Chen C (2015). Inhibition of monoacylglycerol lipase prevents chronic traumatic encephalopathy-like neuropathology in a mouse model of repetitive mild closed head injury. J Cereb Blood Flow Metab *35*, 443-453.

FOOTNOTES

a) All authors are or were formerly employees of Abide Therapeutics.

b) Parts of the manuscript have been previously presented in poster form: J. R. Clapper, J. L. Blankman, A. R. Coppola, A. Knize, G. Simon, J. Cisar, O. Weber, M. Niphakis, C. Henry, I. Fraser, C. Grice, A. Ezekowitz, G. O'Neill. *In vivo* characterization of a selective monoacylglycerol lipase inhibitor ABD-1970 in rodents and activity in models of pain. Program No. 617.02. 2016 Neuroscience Meeting Planner. San Diego, CA: Society for Neuroscience, 2016. Online; J. L. Blankman, C. Henry, A. Knize, G. Simon, J. Cisar, O. Weber, M. Niphakis, J. R. Clapper, A. Coppola, I. Fraser, C. Grice, A. Ezekowitz, G. O'Neill. I*n vitro* characterization of a selective monoacylglycerol lipase inhibitor ABD-1970 in human systems. Program No. 617.03. 2016 Neuroscience Meeting Planner. San Diego, CA: Society for Neuroscience, 2016. Online

c) To whom correspondence should be addressed: Jacqueline L. Blankman. Abide Therapeutics, 10835 Road to the Cure: Suite 250. San Diego CA 92121. USA. jackie@abidetx.com

LEGENDS FOR FIGURES

Figure 1. Chemical structure of ABD-1970 (1,1,1,3,3,3-hexafluoropropan-2-yl 4-(2-(8-oxa-3-azabicyclo[3.2.1]octan-3-yl)-4-chlorobenzyl)piperazine-1-carboxylate).

Figure 2. Potent and selective inhibition of MGLL in brain tissue by ABD-1970. MGLL activity quantitation (A-C) and representative ABPP gels (D-F) in mouse, rat and human brain membrane homogenates treated with ABD-1970 (30 min, 37°C). Mean IC_{50} values are reported in Table 1.

Figure 3. ABD-1970 is highly selective for MGLL in human tissues and cells. Selectivity of ABD-1970 (30 min at 37°C) was evaluated in human tissue and cell homogenates (total homogenates containing soluble and membrane fractions) by gel-based ABPP (A) and in membrane homogenates of human prefrontal cortex by mass spectrometry-based ABPP (B).

Figure 4. ABD-1970 selectively inhibits MGLL in vivo and modulates brain levels of 2-AG, arachidonic acid and prostanoids. ABD-1970 administration (0.1-10 mg/kg, PO, 4 h post-dose, 0.5% methylcellulose vehicle, n=5 rats per group) resulted in selective inhibition of MGLL in the brain (A) with an ED_{50} value of 0.7 mg/kg (B). Dose-dependent increases in brain 2-AG (C) and reductions in brain AA and the prostaglandins PGE_2 and PGD_2 (D) were observed without alterations in brain anandamide concentrations (E). Concentrations of ABD-1970 in brain and blood (F), inhibition of brain MGLL activity (G) and increased 2-AG concentrations were observed following a single oral dose of 12 mg/kg ABD-1970 (PO, n=3 rats per time point, 7:2:1 PEG400:ethanol:PBS vehicle). *$p < 0.05$, **$p < 0.01$, ***$p < 0.001$ vs. vehicle (C,D) or at 0 hour (G,H). Data represent mean ± SEM.

JPET Fast Forward. Published on October 10, 2018 as DOI: 10.1124/jpet.118.252296
This article has not been copyedited and formatted. The final version may differ from this version.

Figure 2. Efficacy of ABD-1970 in the rat formalin model correlates with PK and CNS biomarkers and potentiates analgesic standards of care. (A) Single doses of ABD-1970 (ABD, 1-10 mg/kg, PO) or the positive control pregabalin (PG, 60 mg/kg, PO) administered 4 hours prior to formalin (2.5%, 50 μL, intraplantar), reduced pain behavior measured as total paw licking duration (n=10 rats per group, *p < 0.05, ***p < 0.001 vs. vehicle). (B) Blood and brain concentrations of ABD-1970 measured at the end of the formalin test (~4.75 h post-dose, n=3-10 rats per group), were inversely associated with brain MGLL activity (C) and positively associated with increased 2-AG concentrations (D). (E) The combination of ABD-1970 (ABD, 2 mg/kg, PO, 4 hours pretest) with pregablin (PG, 10 mg/kg, PO, 4 hours pretest) resulted in enhanced antinociceptive activity compared to either agent individually (n=8-10 rats per group, *<0.05, **p<0.01, ***p<0.001 versus vehicle, †††p<0.001 versus PG, ‡‡p<0.01 versus ABD-1970. (F) Combination of ABD-1970 (ABD, 1 mg/kg, PO, 4 hours pretest) with morphine (2.49 mg/kg, SC, 0.5 hours pretest) also resulted in enhanced antinociceptive activity compared to either agent individually (n=9-10 rats per group, *<0.05 versus vehicle, †††p<0.0001 versus morphine). Data represent mean ± SEM.

Figure 6. ABD-1970 demonstrates broad-spectrum antinociceptive and anti-pruritic effects without cannabimimetic effects on locomotor activity. (A-C) Anti-nociceptive effects of ABD-1970 (PO, 0.5% methylcellulose vehicle) in the CFA model of inflammatory pain (A, N=8 rats per group. †p<0.05 vs. ABD-1970 3 mg/kg, †††p<0.001 vs. ABD-1970 3 mg/kg, **p<0.01 vs. ABD-1970 10 mg/kg, ***p<0.001 vs. 10 mg/kg), plantar incision model of acute pain (B, N=8 rats per group. *p<0.05 vs. ABD-1970, ***p<0.001 vs. ABD-1970, ††p<0.01 vs. buprenorphine (Bup), †††p<0.001 vs. buprenorphine), and the CCI model of neuropathic pain (C, N=8-9 rats per group. *p<0.05, **p<0.01 vs. pre-dose). (D) Anti-pruritic effects ABD-1970

(ABD, PO, 0.5% methylcellulose, 4 h pre-test) and naltrexone (NAL, SC, 0.9% saline vehicle, 0.25 h pre-test) in rats following intradermal serotonin administration (N=8 rats per group. ***p<0.001 vs. PO vehicle, †††p<0.001 vs. SC vehicle). (E-G) Behavioral effects of ABD-1970 (PO, 4 h pre-test) or the direct CB1/2 agonist WIN 55,212-2 (WIN, SC, 1% Tween 80/99% saline vehicle, 0.25 h pre-test) on total locomotor duration (E), rearing frequency (F), or grooming (G). (E-G) N=7-8 rats per group, ***p <0.001 vs. vehicle. Data represent mean ± SEM.

Figure 3. MGLL and COX inhibition differentially affect prostanoid production in human cells. The effects of ABD-1970, indomethacin and rofexocib on concentrations of 2-AG, AA and prostanoid lipids were evaluated in human whole blood treated with LPS (A-C) or ionomycin (D and E) or primary HUVEC stimulated with IL-1β (F). In A-C, data are from whole blood from two human donors. In D-F, data are presented as mean ± SEM; *n*=3/group; *p < 0.05, **p < 0.01, ***p < 0.001, ****p < 0.0001 versus stimulated DMSO control. See also Figure S3.

JPET Fast Forward. Published on October 10, 2018 as DOI: 10.1124/jpet.118.252296
This article has not been copyedited and formatted. The final version may differ from this version.

TABLES

Table 1. *In vitro* potency of ABD-1970 against MGLL across species

ABD-1970 (0-10 μM) was pre-incubated with the source material listed for 30 min at 37°C prior to ABPP analysis. Data represent mean ± SEM from several independent experiments. [a] n =4, [b] n=3.

Species	Source	MGLL IC_{50} (μM)
Mouse	Brain[a]	0.015 ± 0.003
Rat	Brain Cortex[b]	0.003 ± 0.001
Rabbit	Brain[b]	0.003 ± 0.001
Dog	Brain Cortex[b]	0.007 ± 0.001
Monkey	Brain Cortex[b]	0.018 ± 0.003
Human	Brain Prefrontal Cortex[b]	0.013 ± 0.003
	PC3 Cell Lysate[a]	0.018 ± 0.003

JPET Fast Forward. Published on October 10, 2018 as DOI: 10.1124/jpet.118.252296
This article has not been copyedited and formatted. The final version may differ from this version.

FIGURES

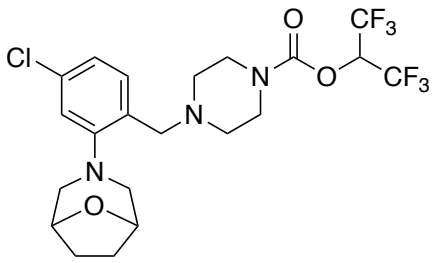

Figure 1. Chemical structure of ABD-1970 (1,1,1,3,3,3-hexafluoropropan-2-yl 4-(2-(8-oxa-3-azabicyclo[3.2.1]octan-3-yl)-4-chlorobenzyl)piperazine-1-carboxylate).

JPET Fast Forward. Published on October 10, 2018 as DOI: 10.1124/jpet.118.252296
This article has not been copyedited and formatted. The final version may differ from this version.

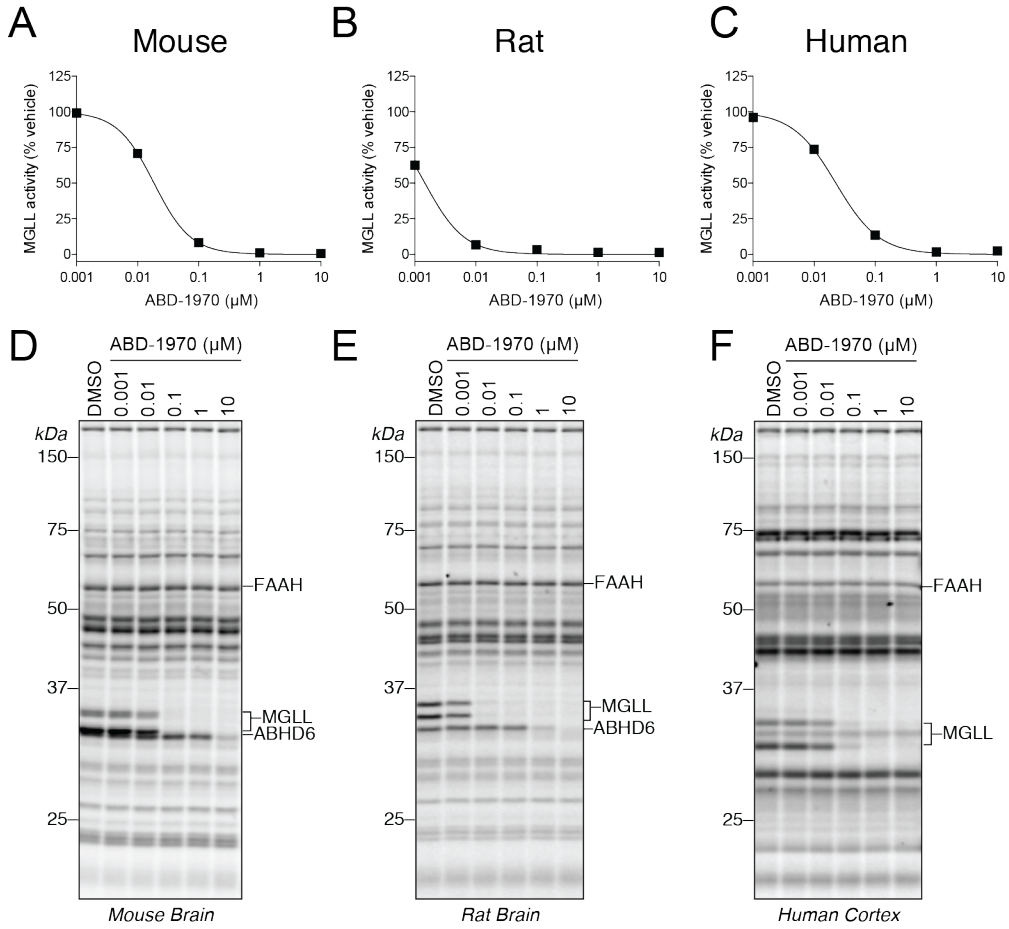

Figure 2.

JPET Fast Forward. Published on October 10, 2018 as DOI: 10.1124/jpet.118.252296
This article has not been copyedited and formatted. The final version may differ from this version.

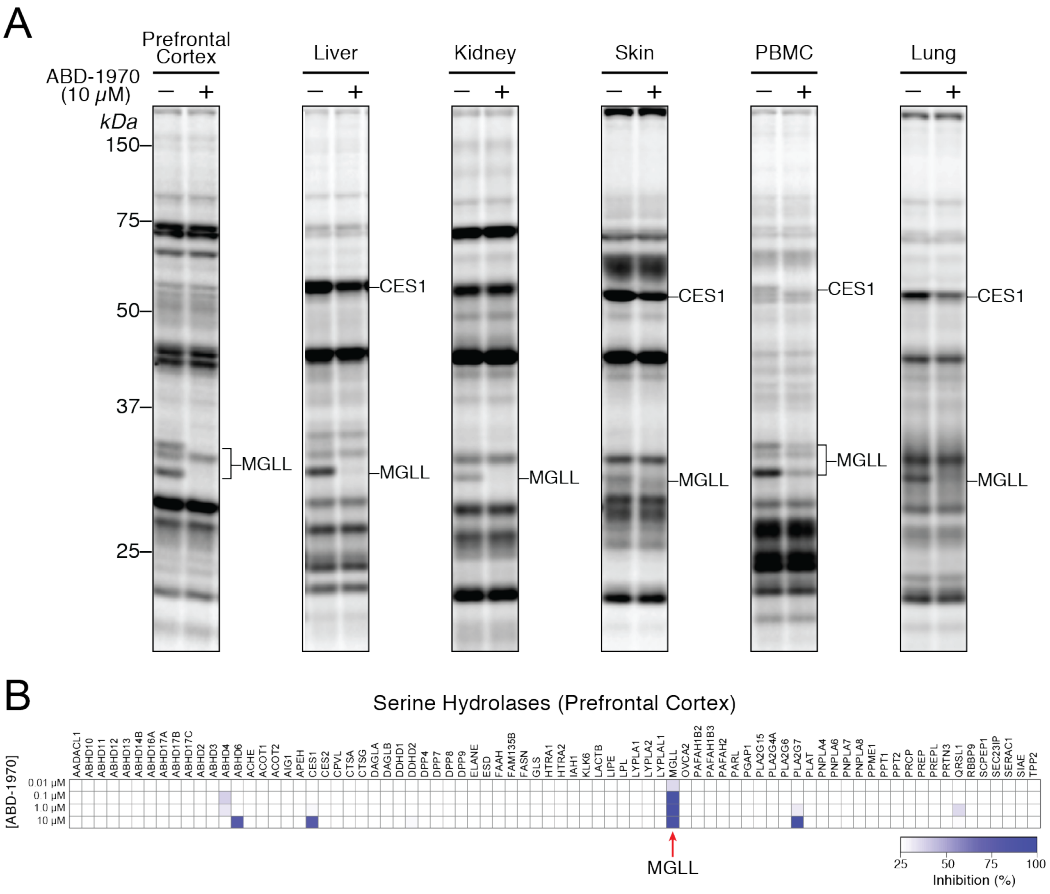

Figure 3.

JPET Fast Forward. Published on October 10, 2018 as DOI: 10.1124/jpet.118.252296
This article has not been copyedited and formatted. The final version may differ from this version.

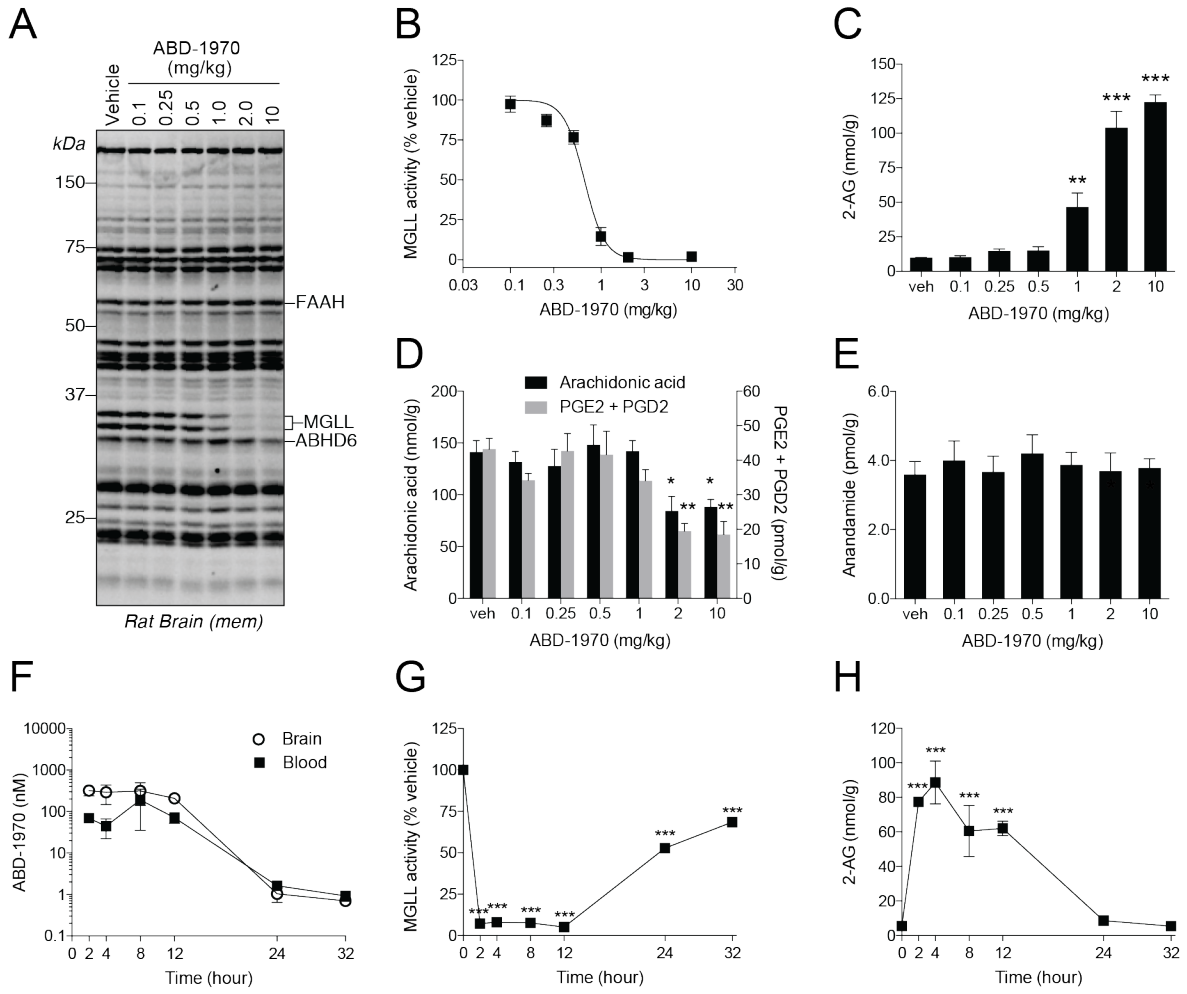

Figure 4.

JPET Fast Forward. Published on October 10, 2018 as DOI: 10.1124/jpet.118.252296
This article has not been copyedited and formatted. The final version may differ from this version.

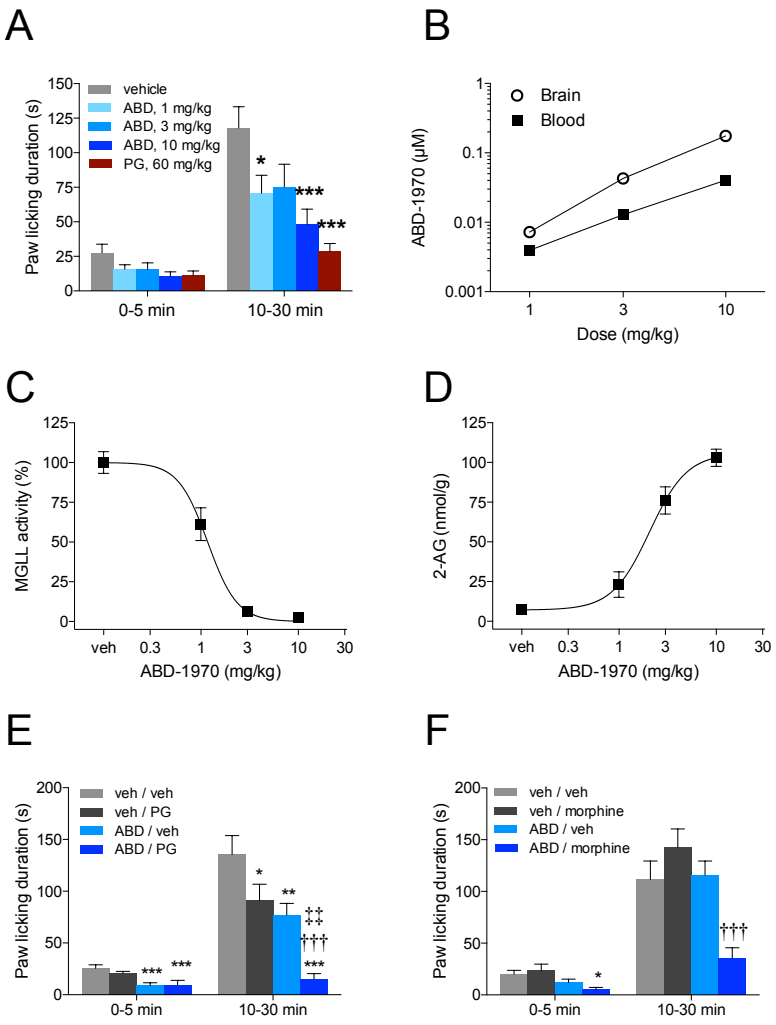

Figure 5.

JPET Fast Forward. Published on October 10, 2018 as DOI: 10.1124/jpet.118.252296
This article has not been copyedited and formatted. The final version may differ from this version.

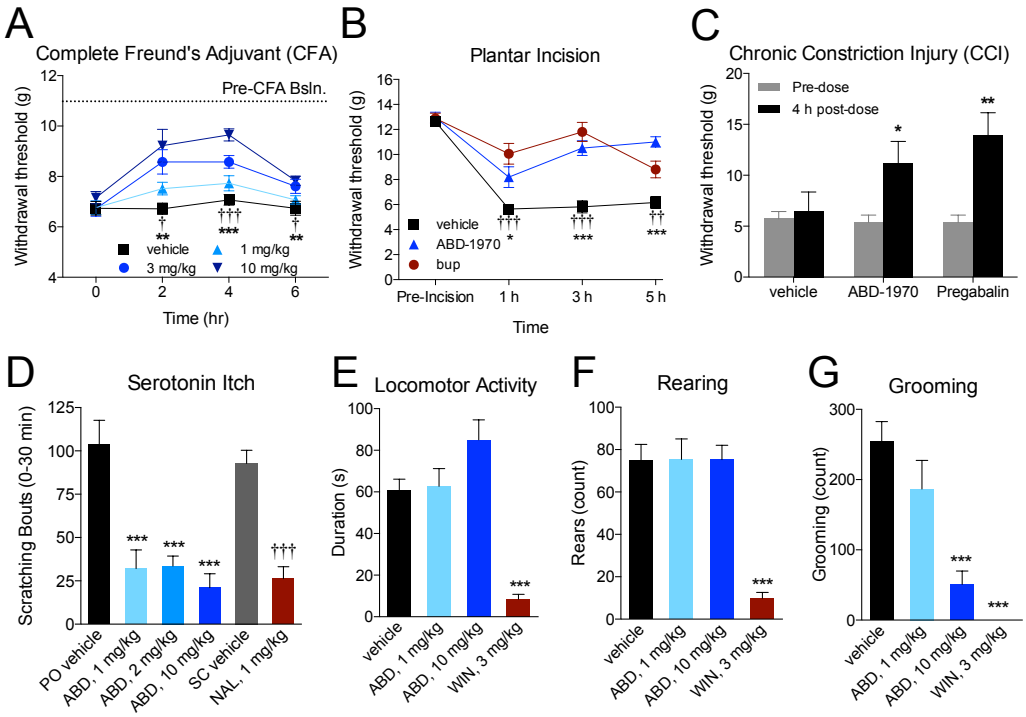

Figure 6.

JPET Fast Forward. Published on October 10, 2018 as DOI: 10.1124/jpet.118.252296
This article has not been copyedited and formatted. The final version may differ from this version.

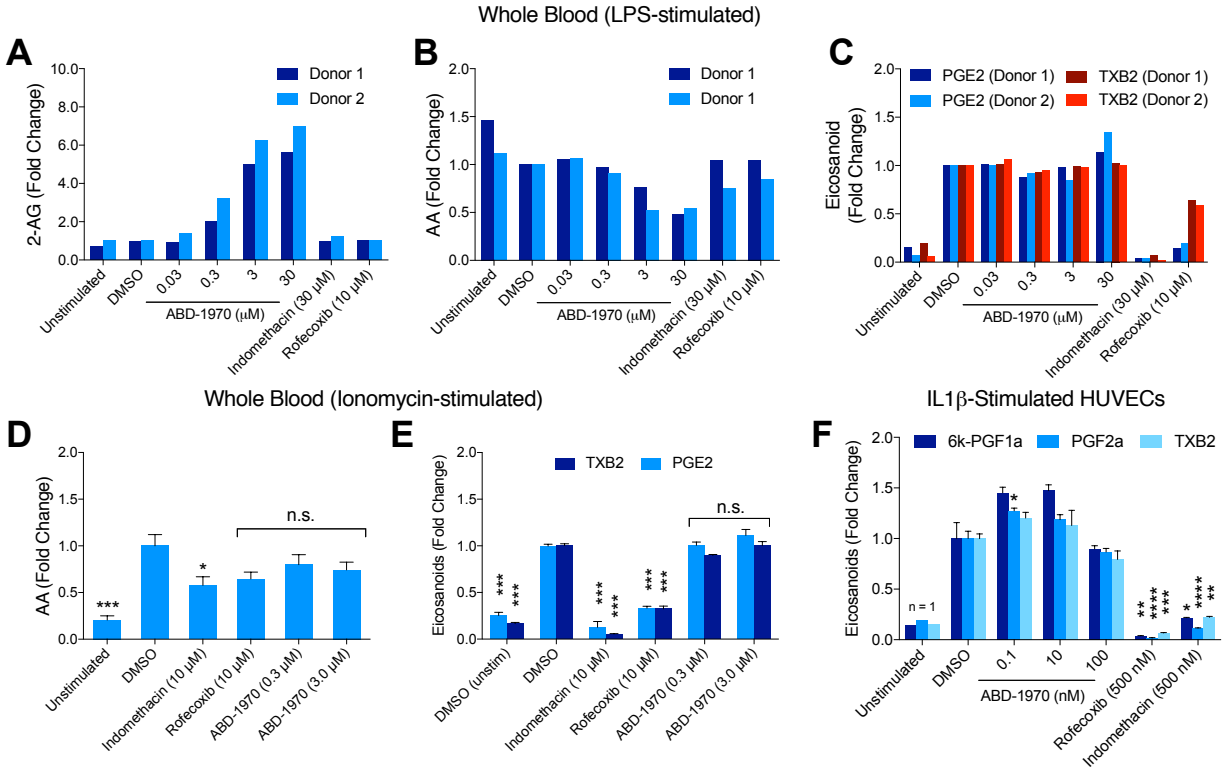

Figure 7.

SUPPLEMENTAL INFORMATION

Monoacylglycerol Lipase Inhibition in Human and Rodent Systems Supports Clinical Evaluation of Endocannabinoid Modulators

Jason R. Clapper, Cassandra L. Henry, Micah J. Niphakis, Anna M. Knize, Aundrea R. Coppola, Gabriel M. Simon, Nhi Ngo, Rachel A. Herbst, Dylan M. Herbst, Alex W. Reed, Justin S. Cisar, Olivia D. Weber, Andreu Viader, Jessica P. Alexander, Mark L. Cunningham, Todd K. Jones, Iain P. Fraser, Cheryl A. Grice, R. Alan B. Ezekowitz, Gary P. O'Neill and Jacqueline L. Blankman*

SUPPLEMENTAL FIGURES

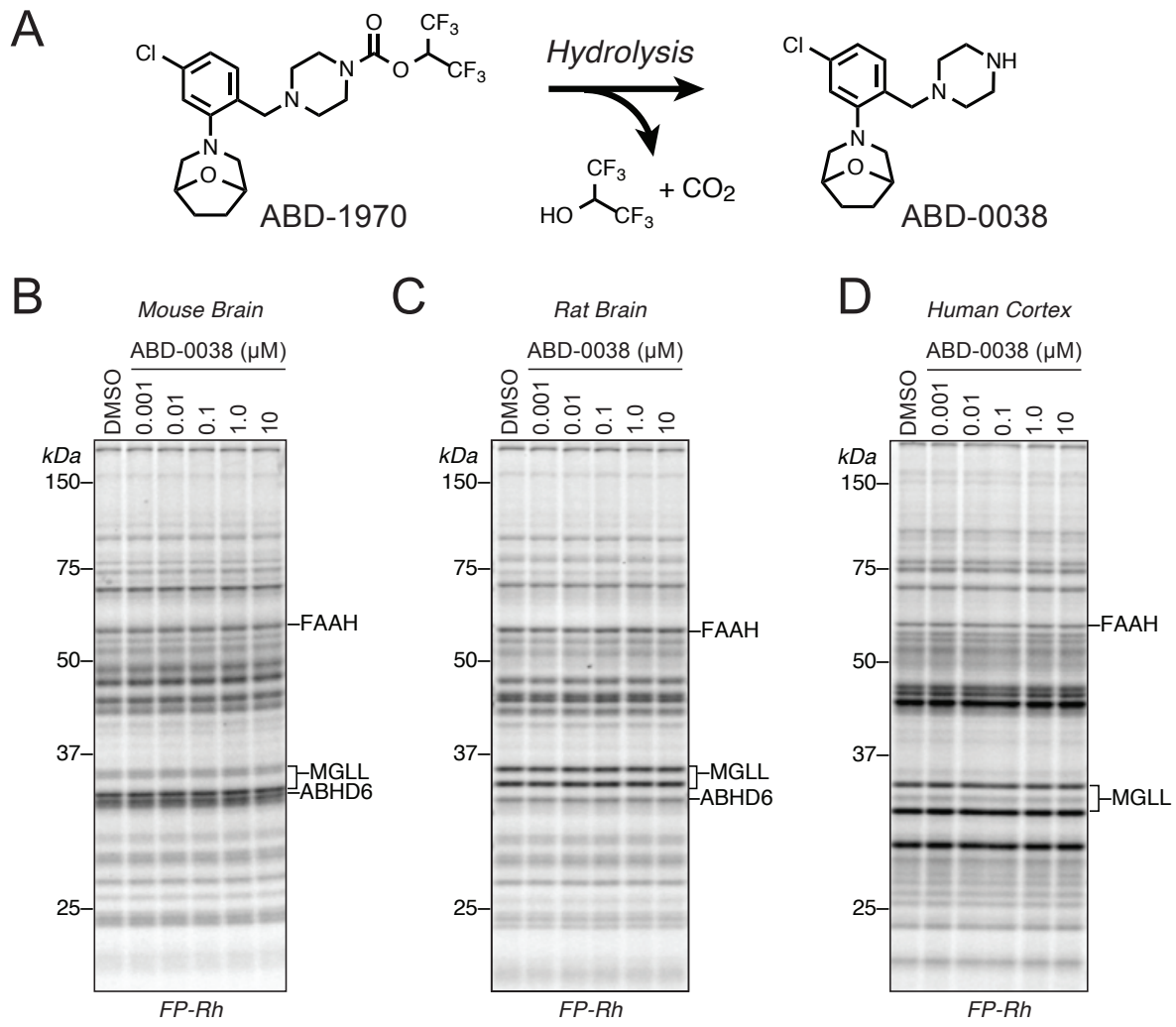

Supplemental Figure 1. In vitro characterization of potential hydrolysis product ABD-0038 by ABPP. (A) ABD-1970 can be potentially hydrolyzed to the amine analog ABD-0038. (B) ABD-0038 (0.001 – 10 μM, 30 min at 37°C) does not inhibit MGLL or any other serine hydrolases in mouse, rat and human brain homogenates as determined by gel-based ABPP with the FP-Rh activity probe.

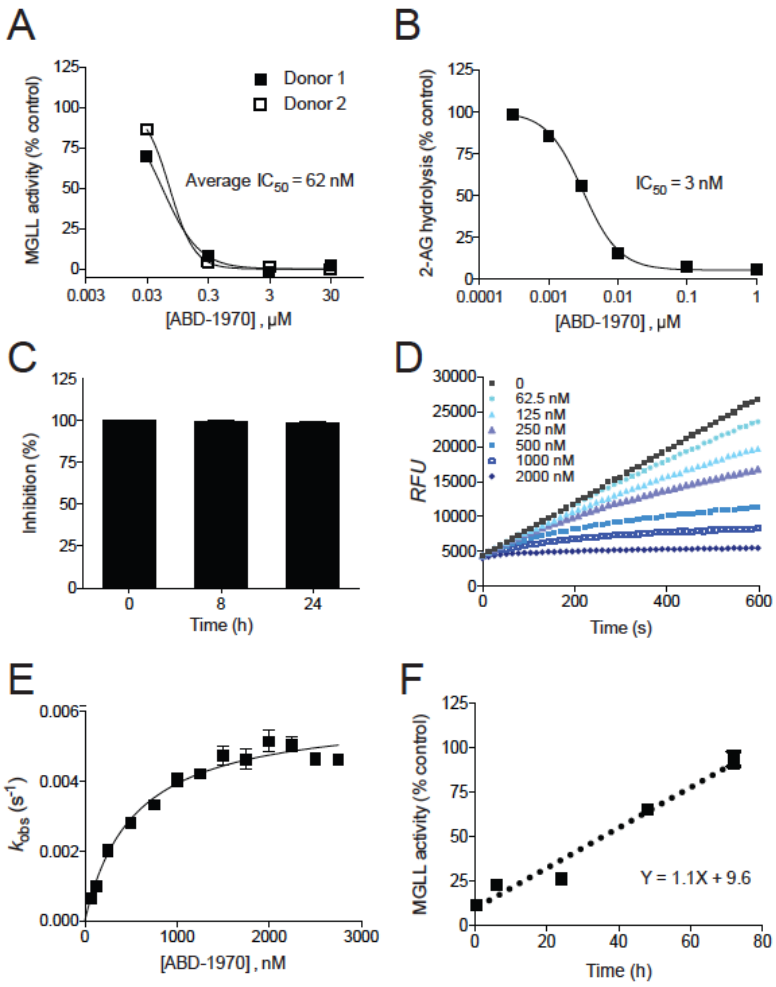

Supplemental Figure 2. In vitro characterization of ABD-1970. (A) ABD-1970 treatment (30 min, 37°C) of human whole blood from two donors inhibited MGLL activity in isolated PBMC with an average IC_{50} value of 62 nM. (B) Treatment of human brain homogenates from a single donor with ABD-1970 (30 min, 37°C) inhibited ~95% of the 2-AG hydrolysis activity with an IC_{50} of 3 nM. (C) Inhibition of MGLL by ABD-1970 persisted for up to 24 h in vitro following removal of unbound inhibitor. (D-E) Purified recombinant hMGLL was treated simultaneously with substrate (butyl resorufin) and ABD-1970, and enzyme activity was monitored continuously by gain in fluorescence upon substrate hydrolysis. The resulting progress curves (representative data shown in D) were fit to a first-order exponential to determine the observed first-order rate constant for enzyme inactivation (k_{obs}) at each concentration of ABD-1970 (representative data shown in E). Non-linear curve fitting of the k_{obs} versus ABD-1970 concentration plot allowed determination of k_{inact}, K_i and the second-order rate constant k_{inact}/K_i. (F) Recovery of MGLL activity was evaluated in cultured human PC3 cells following incubation with ABD-1970 (10 nM, 30 min, 37°C) and removal of unbound compound. Calculation of the average MGLL activity recovery rate was done by linear regression (shown as a black dotted line).

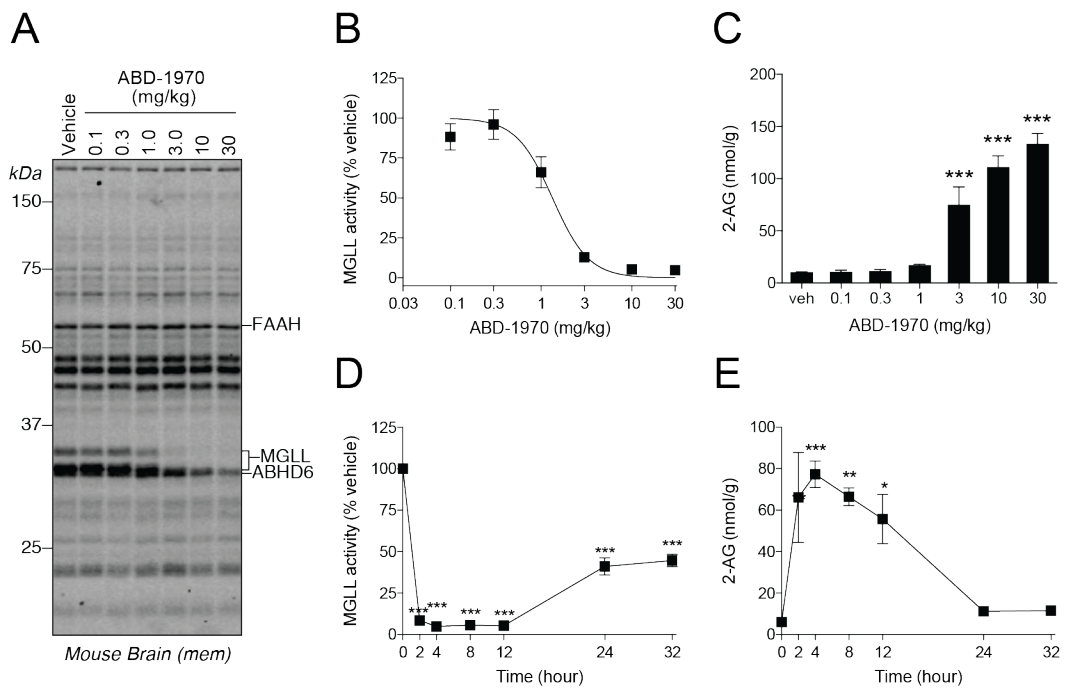

Supplemental Figure 3. Single oral doses of ABD-1970 to mice selectively inhibit MGLL and increase 2-AG concentrations in the brain. The effects of single dose ABD-1970 administration to mice were evaluated across dose (A-C) and time (D, E). ABD-1970 administration (PO, 7:2:1 PEG400/Ethanol/PBS vehicle, 4 h post-dose, n=3 mice per group) resulted in selective inhibition of MGLL in the brain (A) with an ED_{50} value of 1.3 mg/kg (B), and increased brain concentrations of 2-AG (C). A single 10 mg/kg dose of ABD-1970 (7:2:1 PEG400/Ethanol/PBS vehicle) inhibited brain MGLL activity (D) and increased 2-AG concentrations (E) for up to 32 hours post-dose (PO, n=3 mice per time point). *p < 0.05, **p < 0.01, ***p < 0.001 vs. vehicle (C) or 0 hour (D, E). Plotted values represent means ± SEM.

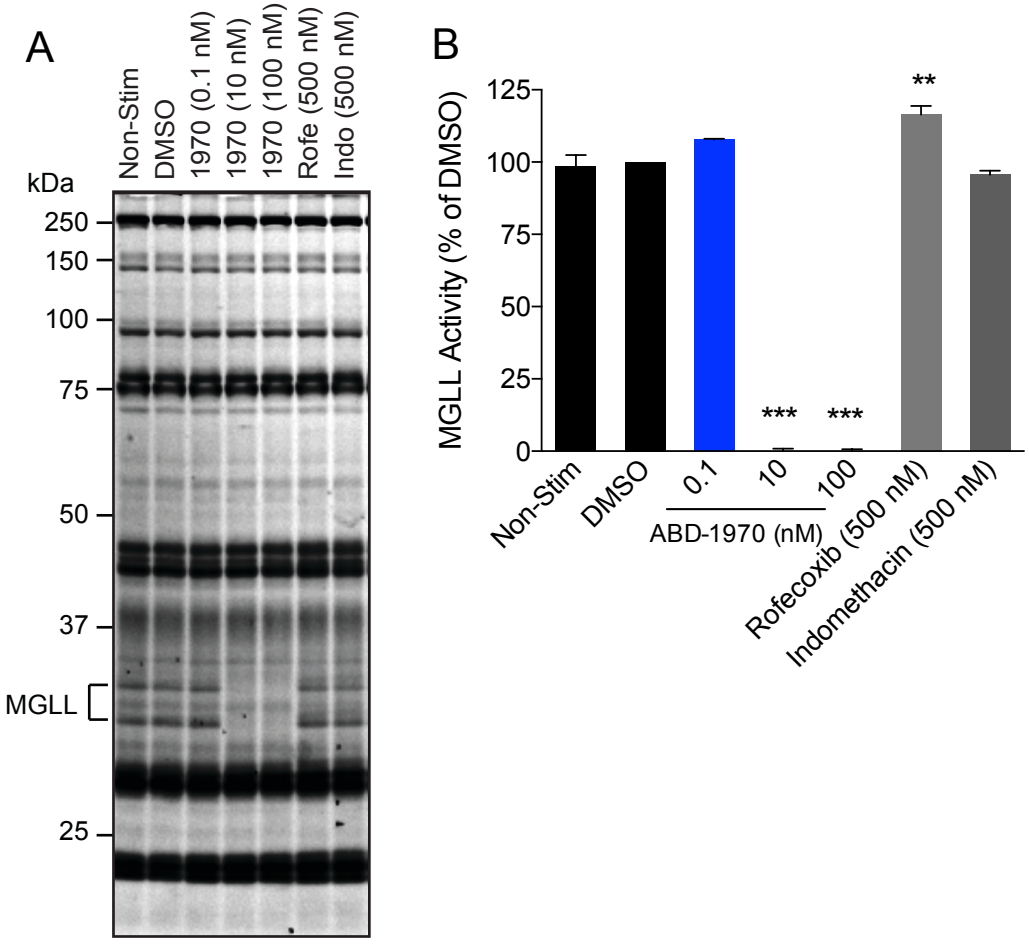

Supplemental Figure 4. Selective MGLL inhibition in ABD-1970-treated HUVEC. MGLL activity in HUVEC was completely inhibited by 10 and 100 nM ABD-1970 treatment (30 min pre-treatment following by 18 h incubation). No additional serine hydrolase targets of ABD-1970 or the other enzyme inhibitors were observed. (B) MGLL activity was quantified from the ABPP gel by densitometry analysis and plotted values represent the mean ± SEM. **p < 0.01, ***p < 0.001 vs. DMSO. Indo, indomethacin; Rofe, rofecoxib.

SUPPLEMENTAL METHODS

Synthesis of ABD-0038: 3-(5-chloro-2-(piperazin-1-ylmethyl)phenyl)-8-oxa-3-azabicyclo[3.2.1]octane.

2-(8-Oxa-3-azabicyclo[3.2.1]octan-3-yl)-4-chlorobenzaldehyde. Commercially available 4-chloro-2-fluorobenzaldehyde (500 mg, 3.15 mmol, 1 equiv) and 8-oxa-3-azabicyclo[3.2.1]octane hydrochloride (566 mg, 3.78 mmol, 1.2 equiv) were combined in a high pressure glass vial with 4 mL DMA and stirred until dissolved. Potassium carbonate (K_2CO_3, 1392 mg, 10.1 mmol, 3.2 equiv) was added and the vial was stirred at 140 °C overnight. The reaction was cooled, diluted with EtOAc (20 mL), and washed with water (4 x 5 mL). Aqueous layers were combined and extracted with EtOAc (3 x 10 mL). The organic layers were combined and dried over Na_2SO_4, decanted and concentrated under reduced pressure to yield an oil which was purified by flash column chromatography to yield 568 mg (71% yield) of 2-(8-oxa-3-azabicyclo[3.2.1]octan-3-yl)-4-chlorobenzaldehyde as a yellow oil. ^{1}H NMR (400 MHz, Chloroform-*d*) δ 10.26 (s, 1H), 7.80 – 7.55 (m, 1H), 7.21 – 6.88 (m, 2H), 4.54 – 4.30 (m, 2H), 3.26 – 3.12 (m, 2H), 3.06 – 2.83 (m, 2H), 2.21 – 1.85 (m, 4H). LCMS (ES, *m/z*): 252 $[M+H]^+$.

tert-Butyl 4-(2-(8-oxa-3-azabicyclo[3.2.1]octan-3-yl)-4-chlorobenzyl)piperazine-1-carboxylate. 2-(8-Oxa-3-azabicyclo[3.2.1]octan-3-yl)-4-chlorobenzaldehyde (568 mg, 2.26 mmol, 1 equiv) was added to a round bottom flask with stir bar, followed by tert-butyl piperazine-1-carboxylate (462 mg, 2.48 mmol, 1.1 equiv) and anhydrous dichloromethane (5 mL). The reaction stirred 1.5 h. Sodium triacetoxyborohydride ($NaBH(OAc)_3$, 526 mg, 2.48 mmol, 1.1 equiv) was added and the reaction was stirred at rt overnight. The reaction mixture was diluted with dichloromethane and filtered over Celite. The organic layers were washed with sat. $NaHCO_3$ (3 x 10 mL), dried

over Na_2SO_4, filtered and concentrated under reduced pressure to yield an oil. The oil was purified by flash column chromatography to yield 455 mg (47% yield) of *tert*-butyl 4-(2-(8-oxa-3-azabicyclo[3.2.1]octan-3-yl)-4-chlorobenzyl)piperazine-1-carboxylate as a clear oil. ^{1}H NMR (400 MHz, Chloroform-*d*) δ 7.41 – 7.32 (m, 1H), 7.10 – 7.03 (m, 2H), 4.44 – 4.35 (m, 2H), 3.59 – 3.49 (m, 2H), 3.46 – 3.35 (m, 4H), 3.07 – 2.99 (m, 2H), 2.87 – 2.80 (m, 2H), 2.43 – 2.33 (m, 4H), 2.16 – 2.08 (m, 2H), 2.03 – 1.91 (m, 2H), 1.47 (s, 9H). LCMS (ES, *m/z*): 422 $[M+H]^+$.

3-(5-Chloro-2-(piperazin-1-ylmethyl)phenyl)-8-oxa-3-azabicyclo[3.2.1]octane. tert-Butyl 4-(2-(8-oxa-3-azabicyclo[3.2.1]octan-3-yl)-4-chlorobenzyl)piperazine-1-carboxylate (377 mg, 0.893 mmol, 1 equiv) was added to a vial with 5 mL anhydrous toluene with stirring. The solution was cooled to 0 °C. 4N HCl in dioxane (3.11 mL, 10.9 mmol, 12.2 equiv) was added drop-wise and the mixture was allowed to stir at rt overnight. The reaction was diluted with methanol and concentrated under reduced pressure to yield an oil which was taken up in EtOAc (30 mL). The organic layer was washed with 5 mL 1N NaOH solution, and the aqueous layer was extracted with EtOAc (3 x 5 mL). Organic layers were combined, dried over Na_2SO_4 and concentrated under reduced pressure to yield 251 mg (87% yield) of *3-(5-chloro-2-(piperazin-1-ylmethyl)phenyl)-8-oxa-3-azabicyclo[3.2.1]octane as a clear oil.* ^{1}H NMR (400 MHz, Chloroform-*d*) δ 7.40 – 7.32 (m, 1H), 7.09 – 6.98 (m, 2H), 4.40 – 4.31 (m, 2H), 3.52 – 3.41 (m, 2H), 3.08 – 2.97 (m, 2H), 2.91 – 2.79 (m, 6H), 2.40 (s, 4H), 2.18 – 2.05 (m, 2H), 2.04 – 1.89 (m, 2H), 1.65 (s, 1H). LCMS (ES, *m/z*): 322 $[M+H]^+$.

Mass spectrometry-based ABPP. Human prefrontal cortex membrane homogenates (1 mg/mL in PBS) prepared as above were treated with 0.01-10 μM ABD-1970 or DMSO for 30 minutes at

37°C. FP-biotin (10 µL of 1 mM in DMSO) was added to a final concentration of 10 µM and incubated for 1 hour at 37°C with gentle rotation. To remove unreacted probe, protein was precipitated by addition of a cold chloroform:methanol (1:4) mixture (2 mL) followed by cold PBS (1.0 mL). Samples were vortexed and centrifuged at 5,000 x g for 15 min resulting in the formation of a protein disc at the interface of the separated organic and aqueous layers. The organic and aqueous layers were removed and the protein disc was resuspended in cold chloroform:methanol (1:4) and dispersed using a waterbath sonicator. The samples were centrifuged at 5,000 x g for 15 min and following removal of the supernatant, the protein pellet was dissolved in a denaturing solution (0.5 mL) containing urea (6.0 M), sodium dodecyl sulfate (SDS) (0.25%), tris(2-carboxyethyl)phosphine (TCEP) (20 mM) and potassium carbonate (60 mM) in PBS with the aid of a waterbath sonicator. The samples were incubated for 30 min at 37°C after which iodoacetamide (70 µL, 55 mM in PBS, Sigma, St Louis, MO) was added and samples were incubated for an additional 30 min at room temperature before diluting with 0.25% SDS in PBS (5.0 mL). PBS-washed streptavidin agarose beads (60 µL, Thermo Fisher Scientific, Waltham, MA) were added to each sample, which were incubated at room temperature for 1.5 hours with gentle rotation. Bead-bound proteins were then sequentially washed with 0.25% SDS (3 x 10 mL), PBS (3 x 10 mL), and distilled water (3 x 10 mL). The beads were then transferred to low-protein binding microcentrifuge tubes, centrifuged, and the supernatant removed by aspiration. Trypsin (1 µg, Promega, Madison, WI) in 2 M urea in PBS was added and samples were incubated overnight at 37°C with shaking. Each sample was centrifuged and the supernatant containing the tryptic peptides were transferred to a new low-protein binding microcentrifuge tube. PBS (100 µL) was added to the beads and they were briefly centrifuged again, and the supernatant combined with the eluate from the previous step.

The inhibitor- and DMSO-treated tryptic peptide samples were isotopically labeled by reductive dimethylation of primary amines with natural or isotopically heavy formaldehydes essentially as previously described (Boersema et al., 2009). Briefly, 10 µL of 4% formaldehyde (CH_2O, "light", DMSO-control) or 4% isotopically heavy formaldehyde ($^{13}CD_2O$, "heavy", ABD-1970-treated) were added directly to tryptic digests and 10 µL of 0.6 M sodium cyanoborohydride ($NaBH_3CN$) (light) was then added to initiate the reaction. Reactions were gently vortexed at room temperature for 1 hour and then quenched by addition of 40 µL of 1% ammonium hydroxide. Appropriate heavy- and light- samples were mixed so that each light DMSO-treated sample was mixed with the corresponding heavy ABD-1970-treated sample. Formic acid (20 µL of 100% formic acid) was added to eluates to acidify peptides. Samples were centrifuged at 17,000 x g for 2 minutes to remove any precipitated protein and the supernatants transferred to fresh tubes and stored at -80°C prior to mass spectrometry analysis.

Liquid chromatography-mass spectrometry and liquid chromatography tandem mass spectrometry (LC-MS/MS) analysis was performed on a a Thermo Fisher (Waltham, MA) Velos Elite Orbitrap mass spectrometer. Peptides were pressure-loaded onto C18 desalting pre-column (~4 cm length, 250 µm ID, Aqua® 5 µm C18 resin) and separated on a biphasic SCX/C18 analytical column (100 µm ID) packed with 3 cm Luna® SCX resin (5 µm) followed by 10 cm Aqua® C18 resin (5 µm). Peptides were eluted using five salt-elution steps (0%, 25%, 50%, 80%, and 100% of 500 mM ammonium acetate) followed by linear acetonitrile gradients. The mass spectrometer was operated in data-dependent acquisition (DDA) mode with a "top 20" method in which the 20 most-abundant MS1 ions are subjected to MS/MS fragmentation in the linear ion trap with dynamic exclusion enabled (repeat count of 1, exclusion duration of 20 s). Peptide spectral matching was performed with the complete human UniProt database using the

ProLuCID algorithm (version 1.3.3) and the resulting matches filtered using DTASelect (version 2.0.47). Quantification of light/heavy ratios was performed using the Cimage algorithm (Weerapana et al., 2010) using a ± 10 ppm mass window and a requirement that heavy/medium and light signals co-elute with a correlation score of $R^2 > 0.8$. The maximum light/heavy ratio was set to 32 and a signal-to-noise ratio greater than 2.5 was required. Calculation of protein ratios required that valid ratios from at least two distinct peptides were observed. Enzyme percent-activity values were derived from the median light/heavy ratio for each protein by setting a ratio of 1 equal to 100% and a maximum ratio of 32 equal to 3.125% active. Data were plotted as percent inhibition relative to DMSO-treated samples.

2-AG hydrolysis assay. Post-mortem human brain cortex membranes (20 μg in 200 μL PBS) were treated with ABD-1970 (0.0003–1 μM) or DMSO vehicle for 30 min at 37°C. Samples were treated with 100 μM of 2-AG at room temperature for 10 min, quenched with 500 μL of 2:1 chloroform:methanol, and 1 nmol pentadecanoic acid (PDA) was added as an internal standard. Reactions were vortexed and centrifuged (1,400 x g for 3 min at room temperature) and a portion of the lower organic phase (10 μL) was isolated for quantitation of AA concentrations by liquid chromatography-mass spectrometry (LC-MS) analysis. Chromatography was performed on an Agilent 1260 liquid chromatography (LC) system with a 50 x 4.60 mm, 5 micron, Kinetex C18 column (Phenomenex, Torrance, CA) coupled to a C18 SecurityGuard ULTRA cartridge (Phenomenex, Torrance, CA). Mobile phase A was 95:5 v/v water:methanol, and mobile phase B was 60:35:5 v/v/v isopropanol:methanol:water. Ammonium hydroxide (0.1% v/v) was added to each mobile phase to aid in negative ion formation. The LC method consisted of 0.5 mL/min 0% B for 1.5 min, a linear gradient to 100% B over 5 min, followed by an isocratic gradient of 100% B for 3.5 min before equilibrating for 3 min at 0% B (13 min total

run time). MS analysis was performed on an Agilent (Santa Clara, CA) 6460C Triple Quadrupole mass spectrometer with a Jet Stream electrospray ionization (ESI) source in single ion monitoring (SIM) mode. The following parent m/z values were tracked: PDA 241.3 and AA 303.3. The capillary voltage was set to 3.5 kV with 2 kV nozzle voltage. The fragmentor voltage was set to 100 V and the DeltaEMV- was 200. The drying gas temperature was 350°C, the drying gas flow rate was 10 L/min, the nebulizer pressure was 35 psi, the sheath gas temperature was 375°C, and the sheath gas flow rate was 10 L/min. The amount of AA product formed by 2-AG hydrolysis was determined from the area under the peak of the extracted ion chromatogram relative to the internal PDA standard. An IC_{50} was calculated for inhibition of 2-AG hydrolysis by ABD-1970 treatment by curve-fitting the normalized (to percent of DMSO vehicle) and semi-log-transformed data (x-axis) with Prism software (GraphPad, La Jolla, CA) by non-linear regression with a sigmoidal dose response function (variable slope).

Quantitation endocannabinoid and eicosanoid lipids in brain tissue. Frozen brain tissue from mouse (sagittally-sectioned half brain) or rat (~100 mg of forebrain) were weighed and immediately homogenized using a Dremel Tissue Tearor (Biospec, Cole Parmer, Vernon Hills, IL, Model 985370) in 8 mL of 2:1:1 chloroform ($CHCl_3$):methanol (MeOH):PBS pH 7.5 acidified with 40 µL of formic acid and containing the following deuterated internal standards: 100 pmol anandamide-d_4, 1.0 nmol 2-AG-d_5, 1.0 nmol arachidonic acid-d_8 (AA-d_8), 100 pmol PGE_2-d_9, and 100 pmol Prostaglandin D2-d4 (PGD_2-d_4). Homogenates were centrifuged at 1,290 x g for 5 min at 4°C and the organic (lower) layer was isolated, transferred to a glass vial and dried under a stream of N_2. Dried down lipid extracts were resuspended in 500 µL 2:1 $CHCl_3$:MeOH, and 10 µL of each sample were injected onto an Agilent (Santa Clara, CA) 1260 LC system. Chromatography was performed on a 30 x 50mm, 2.7 micron, InfinityLab Poroshell

C18 column (Agilent, Santa Clara, CA) coupled to an InfinityLab Poroshell 120 EC-C18, 3x5 mm, 2.7 μm guard column (Agilent, Santa Clara, CA). The LC method consisted of 0.4 mL/min 100% Buffer A from 0 min to 2 min, 0.4 mL/min linear gradient from 40-100% Buffer B from 2 min to 9 min, 0.5 mL/min 100% Buffer B from 9 min to 12 min, and 0.5 mL/min 100% Buffer A from 12 min to 13 min, 0.5mL/min 100% Buffer B from 13 min to 15 min, 0.4 mL/min 100% Buffer A from 15 min to 17 min (17 min total run time per sample). Buffer A consisted of 95:5 (v/v) H_2O:MeOH and Buffer B consisted of 60:35:5 (v/v/v) isopropanol ([iPrOH]:MeOH:H_2O). To each buffer, 0.1% formic acid was added to aid in ion formation. An Agilent (Santa Clara, CA) Triple Quadrupole 6460 mass spectrometer with an ESI-Jet Stream source was used to measure analytes by dynamic multiple-reaction-monitoring (MRM) in both positive and negative ionization mode. The following MS parameters were used to measure the indicated lipids (precursor ion, product ion, collision energy in V, polarity): 2-AG (379, 287, 8, Positive), 2-AG-d_5 (384, 287, 8, Positive), anandamide (348.3, 62.1, 11, Positive), anandamide-d_4 (352.3, 66.1, 11, Positive), PGE_2/D_2 (351, 271, 4, 7, Negative), PGE_2-d_9 (360, 280, 4, 7, Negative), AA (303, 303, 0, Negative), and AA-d_8 (311, 311, 0, Negative). The fragmentor voltage was set to 100 V, and the delta EMV was ±500. The drying gas temperature was 350 °C, the drying gas flow rate was 9 L min^{-1}, the nebulizer pressure was 50 psi, the sheath temperature was 375°C, the sheath flow was 12 L min^{-1}, the capillary was 3.5 kV. Lipids were quantified by measuring the area under the peak in comparison to the deuterated internal standards.

Quantitation endocannabinoid and eicosanoid lipids in human plasma and HUVEC media.
Frozen plasma or HUVEC media was thawed (37°C, water bath) and immediately placed on ice. Thawed plasma (0.5 or 1 mL) was diluted with 10% methanol (MeOH) in water (1.5 mL) whereas thawed HUVEC media was used directly. To these solutions were added a mixture of

internal standards containing 0.5 nmol d_5-2-AG, 1.0 nmol d_8-arachidonic acid (d_8-AA), 27.7 pmol d_9-PGE_2, 27.7 pmol, d_9-PGD_2, 27.9 pmol d_4-$PGF_{2\alpha}$, 26.7 pmol d_4-6-keto-$PGF_{1\alpha}$ and 26.7 pmol d_4-Thromboxane B2 (d_4-TXB_2) in a solution of 1:1 MeOH:water (100 µL). Samples were loaded onto methanol-washed, pre-equilibrated reversed phase SPE cartridges (Phenomenex, Strata-X 33 µm, 60 mg/3mL). After washing cartridges with 10% MeOH in water (3 mL), prostanoids were eluted into glass vials with methanol (1.0 mL) and the eluent was concentrated under a stream of N_2. Concentrated samples were stored at –80°C until the day of analysis when they were reconstituted in Buffer A [100 µL, 30% acetonitrile in water (0.1% AcOH)].

From each sample, 20 µL was injected onto an Agilent 1260C system. Chromatography was performed on a Phenomenex Kinetix™ C18 (50 x 2.1 mm) LC column (2.6 µm particle size, 100 Å pore size) coupled to a C18 SecurityGuard ULTRA cartridge (Phenomenex, Torrance, CA). The LC method consisted of 0.30 mL/min 100% Buffer A for 2.5 min, 0.35 mL/min linear gradient from 0-20% Buffer B over 2.5 min, 0.35 mL/min 20% Buffer B for 2 min, 0.35 mL/min linear gradient from 20-75% Buffer B over 5 min, 0.35 mL/min linear gradient from 75-100% Buffer B over 3 min and 0.35 mL/min 100% Buffer A for 3 min. Buffer A was finally returned to 100 % at 0.30 mL/min for 2 min yielding a 20 min total run time per sample. Buffer A consisted of 70:30 (v/v) water:acetonitrile and Buffer B consisted of 60:35:5 (v/v/v) isopropanol (iPrOH):methanol:water). To each buffer formic acid was added to achieve a final concentration of 0.1% (v/v) to aid separation and ion formation.

An Agilent (Santa Clara, CA) Triple Quadrupole 6460 mass spectrometer with an ESI-Jet Stream source was used to measure analytes by dynamic MRM in both positive and negative ionization mode. The following MS parameters were used to measure the indicated species

(precursor ion, product ion, collision energy in V, retention time in min, polarity): 2-AG (379, 287, 8, 14.3, Positive), d_5-2-AG (384, 287, 8, 14.3, Positive), PGD_2 (351, 271, 12, 6.4, Negative), d_9-PGD_2 (360, 280, 12, 6.4, Negative), PGE_2 (351, 271, 4, 7, Negative), d_9-PGE_2 (360, 280, 4, 7, Negative), $PGF_{2\alpha}$ (353, 193, 12, 5.6, Negative), d_4-$PGF_{2\alpha}$ (357, 197, 12, 5.6, Negative) Thromboxane B2 (TXB_2) (369, 169, 6, 4.5, Negative), d_4-TXB_2 (373, 173, 6, 4.5, Negative), 6k-$PGF_{1\alpha}$ (369, 163, 20, 2.6, Negative), d_4-6k-$PGF_{1\alpha}$ (373, 167, 20, 2.6, Negative), AA (303, 303, 0, 15, Negative), d_8-AA (311, 311, 0, 15, Negative). The fragmentor voltage ranged set between 80 and 160 V, and the delta electromagnetic voltage was ±400. The drying gas temperature was 300 °C, the drying gas flow rate was 9 L min^{-1}, the nebulizer pressure was 45 psi, the sheath temperature was 300°C, the sheath flow was 12 L min^{-1}, the capillary was 3.5 kV. Lipid levels were quantified by integrating the corresponding peak from the extracted ion chromatogram in comparison to the corresponding deuterated internal standard.

SUPPLEMENTAL REFERENCES

Boersema PJ, Raijmakers R, Lemeer S, Mohammed S, and Heck AJ (2009). Multiplex peptide stable isotope dimethyl labeling for quantitative proteomics. Nat Protoc *4*, 484-494.

Weerapana E, Wang C, Simon GM, Richter F, Khare S, Dillon MB, Bachovchin DA, Mowen K, Baker D, and Cravatt BF (2010). Quantitative reactivity profiling predicts functional cysteines in proteomes. Nature *468*, 790-795.